Check for updates

the plant journal

SEB SOCIETY FOR EXPERIMENTAL BIOLOGY

*The Plant Journal* (2024) doi: 10.1111/tpj.16742

# The outstanding capacity of *Prasiola antarctica* to thrive in contrasting harsh environments relies on the constitutive protection of thylakoids and on morphological plasticity

**Miren I. Arzac[1,*], Jon Miranda-Apodaca[1], Asunción de los Ríos[2], Francesc Castanyer-Mallol[3], José I. García-Plazaola[1] and Beatriz Fernández-Marín[1,4]**

[1]*Department of Plant Biology and Ecology, University of the Basque Country (UPV/EHU), Barrio Sarriena s/n, 48940 Leioa, Spain,*

[2]*Museo Nacional de Ciencias Naturales (MNCN-CSIC), Serrano 115 dpdo, 28006 Madrid, Spain,*

[3]*Research Group on Plant Biology under Mediterranean Conditions, Department of Biology, Universitat de les Illes Balears (UIB), INAGEA, Balearic Islands, Palma, Spain, and*

[4]*Department of Botany, Ecology and Plant Physiology, University of La Laguna (ULL), Canary Islands, 38200 La Laguna, Spain*

Received 26 March 2023; revised 29 February 2024; accepted 14 March 2024.
*For correspondence (e-mail mirenirati.arzac@ehu.eus).

## SUMMARY

**The determination of physiological tolerance ranges of photosynthetic species and of the biochemical mechanisms underneath are fundamental to identify target processes and metabolites that will inspire enhanced plant management and production for the future. In this context, the terrestrial green algae within the genus *Prasiola* represent ideal models due to their success in harsh environments (polar tundras) and their extraordinary ecological plasticity. Here we focus on the outstanding *Prasiola antarctica* and compare two natural populations living in very contrasting microenvironments in Antarctica: the dry sandy substrate of a beach and the rocky bed of an ephemeral freshwater stream. Specifically, we assessed their photosynthetic performance at different temperatures, reporting for the first time $g_{nsd}$ values in algae and changes in thylakoid metabolites in response to extreme desiccation. Stream population showed lower α-tocopherol content and thicker cell walls and thus, lower $g_{nsd}$ and photosynthesis. Both populations had high temperatures for optimal photosynthesis (around +20°C) and strong constitutive tolerance to freezing and desiccation. This tolerance seems to be related to the high constitutive levels of xanthophylls and of the cylindrical lipids di- and tri-galactosyldiacylglycerol in thylakoids, very likely related to the effective protection and stability of membranes. Overall, *P. antarctica* shows a complex battery of constitutive and plastic protective mechanisms that enable it to thrive under harsh conditions and to acclimate to very contrasting microenvironments, respectively. Some of these anatomical and biochemical adaptations may partially limit photosynthesis, but this has a great potential to rise in a context of increasing temperature.**

**Keywords: tolerance, plasticity, *Prasiola antarctica*, photosynthesis, morphology, desiccation, freezing, trigalactosyldiacylglycerol, Antarctica.**

## INTRODUCTION

Light, temperatures and water availability are the main constraints to photosynthesis worldwide (Boisvenue & Running, 2006). In extreme environments, an orchestrated arrangement of morpho/anatomical, photochemical and metabolic adaptive processes enable the positive carbon balance of photosynthetic organisms under severe conditions (Fernández-Marín, Gulías, et al., 2020). In addition to anatomical and physiological adaptations, some photosynthetic organisms living in harsh environments show an outstanding capacity of acclimation and are able to display a wide range of ultrastructural and biochemical adjustments. This is, for instance, the case of the desert green algae *Chlorella ohadii* which massively adjust PSII antenna size according to the growing light intensities (Levin et al., 2021). In this context, an efficient photoprotection of the photosynthetic machinery is essential to succeed (Fernández-Marín, Gulías, et al., 2020). Interestingly,

© 2024 The Authors.
*The Plant Journal* published by Society for Experimental Biology and John Wiley & Sons Ltd.
This is an open access article under the terms of the Creative Commons Attribution License, which permits use, distribution and reproduction in any medium, provided the original work is properly cited.

sub-zero temperatures and severe desiccation share many protective physiological requirements, particularly those related to photoprotection (Verhoeven et al., 2018). Thus, an efficient management of the excess light energy absorbed by chlorophylls that cannot be transferred to photochemistry under sub-zero or low water content of the tissues is crucial. In that sense, a large pool of the carotenoids involved in the so-called xanthophyll cycle, with relevant roles in excess energy dissipation, thylakoid membrane stabilisation and as antioxidants, seems to be determinant in environments with high photoprotective demand such as polar tundra (Fernández-Marín, Atherton, et al., 2018; Fernández-Marín, Gago, et al., 2019; Magney et al., 2017; Schroeter et al., 2012). Fast and dynamic de-epoxidation of the violaxanthin into the protective zeaxanthin within the xanthophyll cycle, in response to either increasing irradiance, sub-zero temperatures or severe desiccation, it is equally relevant for suitable photoprotection of the photosynthetic machinery in species tolerant to either desiccation, intra-tissular ice formation, or both (Fernández-Marín, Arzac, et al., 2021; Fernández-Marín, Neuner, et al., 2018) and for species in polar tundra too (Fernández-Marín, Gago, et al., 2019; García-Plazaola, López-Pozo, & Fernández-Marín, 2022). The fine tuning and responsiveness of the xanthophyll cycle to the environmental conditions acquires even more relevance when considering that too slow re-epoxidation of zeaxanthin back to violaxanthin represents an important payback for net photosynthesis estimated in a 20% reduction for crop-plants (Kromdijk et al., 2016). Despite efforts being made in that sense in the few recent years, and probably due to the logistical difficulties to get these data, *in situ* studies of xanthophyll cycle dynamism are rather scarce for high latitudes. As an example, after compiling more than 500 studies about photosynthetic pigment composition (Esteban et al., 2015) none of the works was performed at latitudes higher than 67° and only thre at latitudes above 60°.

At thylakoid level, another group of relevant molecules in the photosynthesis–stress tolerance 'trade off' are the polar lipids that constitute chloroplast membranes, as well as their post-synthetic structural modifications (Yu et al., 2021). The nature of their head group, but also the length and the degree of saturation of their acyl chains, determine the physical, and thus functional, properties of the membranes: fluidity, permeability, bilayer thickness, charge and intrinsic curvature. Galactolipids (GLs) are, in particular, the main lipids in chloroplast membranes and, consequently, are also the most abundant polar lipids on Earth (Rolland et al., 2009). Among them, GLs with one or two galactose residues, monogalactosyldiacylglycerol (MGDG) and digalactosyldiacylglycerol (DGDG), are ubiquitous and essential for photosynthesis. On the other hand, GLs containing three or higher numbers of galactose residues (so-called oligogalactolipids) are only known for some specific taxa, organs and environmental conditions (Gasulla et al., 2019). While MGDGs (which are conical-shaped molecules), confer fluidity to the thylakoid membranes and are essential for photosynthetic functions, DGDGs and oligocalactolipids (OGLs) (are cylindrical molecules) conferring rigidity and stability to the thylakoids. Very likely, the appearance of OGLs was one of the adaptations that simultaneously provided advantages against environmental constraints such as desiccation and freezing during land colonisation by plants (Gasulla et al., 2019). Unfortunately, very few studies have addressed the composition and stress responses of OGLs (reviewed in Gasulla et al., 2019) and, to the best of our knowledge, just a few works are available for Chlorophyte species, so far (Benson et al., 1958; Gasulla et al., 2016; Mendiola-Morgenthaler et al., 1985; Montero et al., 2021; Vieler et al., 2007).

Overall, all these physiological adaptations and acclimation capabilities had to evolve during terrestrialisation. The process of terrestrialisation occurred simultaneously in the two lineages of green algae: streptophytes and chlorophytes (Leliaert et al., 2012). While the streptophytes gave rise to land plants, several clades of the chlorophytes adapted to a fully terrestrial life. This is, for instance, the case of the genus *Fritschiella* among the class Chlorophyceae or the genus *Trentepohlia* among the class Ulvophyceae (Holzinger & Karsten, 2013). It is, however, in the class Trebouxiophyceae where the adaptation to terrestrial life spread more widely. Trebouxiophyceae comprises unicellular species including free-living taxa such as *Chlorella* (Aigner et al., 2020) and symbiotic lichen-forming taxa such as *Trebouxia* (Muggia et al., 2018). Exceptional within the class, for having a multicellular, macroscopic blade-like thallus is the genus *Prasiola* (Sanders & Masumoto, 2021), which is worldwide distributed and particularly abundant in Polar and cold-temperate regions (Rindi et al., 2007). *Prasiola* species show a remarkable ecological plasticity and stress tolerance and comprise freshwater, supralitoral and aeroterrestrial species (Holzinger et al., 2017; Huiskes et al., 1997; Kang et al., 2013; Moniz et al., 2012; Ramírez et al., 2007; Zębek et al., 2021). Thus, physiological and/or structural responses to desiccation tolerance have been examined from urban environments (Holzinger et al., 2017), from Arctic supralittoral sites (Kang et al., 2013) and from Antarctica (Bacior et al., 2017; Fernández-Marín, López-Pozo, et al., 2019; Huiskes et al., 1997; Jacob, Wiencke, et al., 1992). Several species show high physiological plasticity to acclimate to wide ranges of salinity (Jacob et al., 1991; Jacob, Lehmann, et al., 1992). Most species are well photoprotected against UV-radiation (Hartmann et al., 2016; Lud et al., 2001) and against excess of visible radiation too (Kosugi et al., 2020). The species with polar distribution are additionally highly tolerant to freezing (Bacior et al., 2022; Fernández-Marín, López-Pozo, et al., 2019) and very frequently

© 2024 The Authors.


1365313x, 0, Downloaded from https://onlinelibrary.wiley.com/doi/10.1111/tpj.16742 by Institution Nac De Investig Tec Agra, Wiley Online Library on [24/05/2024]. See the Terms and Conditions (https://onlinelibrary.wiley.com/terms-and-conditions) on Wiley Online Library for rules of use; OA articles are governed by the applicable Creative Commons License

associated with nitrogen-rich deposits (Abakumov et al., 2021; Holzinger et al., 2006; Lud et al., 2001).

Notably, green algae species of the genus *Prasiola* are widely distributed at many terrestrial and supralittoral sites (Broady, 1989), being especially abundant near ornithogenic soils (Abakumov et al., 2021; Smith & Gremmen, 2001) and, even though their production rate is lower than the one of mosses (the main primary producers in Antarctica together with lichens), they are important food sources and habitat for primary consumers along with microflora (Davis, 1981; Lukashanets et al., 2022). Thanks to molecular markers (plastid genes *tufA* and *rbc*L), the taxonomy of Antarctic *Prasiola* species has recently been re-examined by several authors (Dubrasquet et al., 2021; Garrido-Benavent et al., 2017; Moniz et al., 2012; Pellizzari et al., 2017). At least four distinct species (*P. crispa*, *P. borealis*, *P. glacialis* and *P. antarctica*) have been reported in Antarctica together with other undescribed species (*Prasiola* sp.) (Garrido-Benavent et al., 2017). Overall, they inhabit the three main biogeographic regions of the continent: i.e. Eastern Antarctica (Kappen et al., 1998; Lukashanets et al., 2021), West Antarctica (Moniz et al., 2012) and Maritime Antarctica (Dubrasquet et al., 2021; Fernández-Marín, López-Pozo, et al., 2019; Garrido-Benavent et al., 2017). *P. crispa* and *P. borealis* lichenised with the fungus *Mastodia tessellate* appear on sea-shore rocks (Fernández-Marín, López-Pozo, et al., 2019; Garrido-Benavent et al., 2018; Pérez-Ortega et al., 2010; Smith & Gremmen, 2001). However, the free-living *Prasiola* species are the most conspicuous and occupy different habitats in Antarctica. The Antarctic *Prasiola* species dominate the vegetation in the vicinity of seabird colonies (Abakumov et al., 2021), flourishing in the so-called ornithogenic soils (strongly influenced by the supply of nitrogen and organic matter) (Durán et al., 2021). Some populations occur in temporal streams (Moniz et al., 2012) and have also been found in extremely harsh environments such as McMurdo Dry Valleys (Moniz et al., 2012).

In this work we selected two populations of *P. antarctica* living on two relatively close areas in Livingston Island, Maritime Antarctica, but in extremely contrasting habitats (an ephemeral freshwater stream on the one hand and a supralittoral and terrestrial environment on a rocky beach). We hypothesise that plasticity, in both morphological and physiological terms, may enable this Antarctic endemism species to be successful in such harsh and contrasting environments. Specifically, we compare the main anatomical features of their thalli, their photosynthetic performance at different temperatures, their freezing and desiccation tolerances and the physiological responses of thylakoid membranes against severe dehydration between both populations.

## RESULTS

### Characterisation of the two studied populations of *P. antarctica*

Figures 1 and 2 depict, respectively, the study site including the location of the two studied populations and the main meteorological conditions during field-work in the vicinity of the 'Base Antarctica Española Juan Carlos I (BAE JCI)' Research station. *rbc*L and *tufA* gene sequences recovered from the two *Prasiola* populations confirmed that they corresponded to the same species (same sequences were obtained for both populations) which could be assigned to *P. antarctica*. *rbc*L sequence matched 99.74% with *P. antarctica* (JQ669721.1) and *tufA* sequence 99.84% with *P. antarctica* (KF993447.1) in NCBI BLAST searches confirming their identity. Figure 3 and Table 1 show general morphological and anatomical aspects of the two studied populations. Henceforth, population from *Site 1* will be referred to as '*P. antarctica* pop. Beach' and population from *Site 2* as '*P. antarctica* pop. Stream' (Figure 1). *P. antarctica* pop. Beach formed dense masses very barely attached to the substrate on a supralittoral belt (Figures 1d and 3a). Its thallus had foliose habit and showed big cells ($11.8 \pm 0.2$ μm high and $4.3 \pm 0.2$ μm width; Figure 3b,c; Table 1). The cells were arranged in clear areolae delimited by thickened borders from a surface view (Figure 3b). By contrast, *P. antarctica* pop. Stream thalli were attached to stones on the bed of the stream and showed a filamentous habit (Figure 3e). The cells were smaller and with thicker cell walls ($2.8 \pm 0.2$ μm) than those of pop. Beach (Figure 3f,g; Table 1). Photosynthetic pigment composition of both populations was rather similar. Content of chlorophyll (Chl) *a* was slightly higher at the beach population although not significantly (Figure 3d,h). The Chl *a/b* ratio (mol/mol) was $2.053 \pm 0.039$ for Stream population and $2.22 \pm 0.056$ for the Beach population ($P = 0.096$).

### Photosynthetic performance

The photosynthetic performance of both populations was analysed under different temperature conditions. Based on the light curves of net $CO_2$ assimilation ($A_N$) performed at +4°C (Figure S1), an irradiance of 500 μmol $m^{-2}$ $s^{-1}$ photosynthetic photon flux density (PPFD) ($A_{N500}$) was selected for the posterior measurements. Under these conditions, *P. antarctica* pop. Beach and Stream showed comparably low assimilation values (<1 μmol $CO_2$ $m^{-2}$ $s^{-1}$; Table 1), but temperature had a significant rising effect for both populations (Figure 4A,B). Lowest $A_{N500}$ was actually obtained at +4°C for both *P. antarctica* pop. Beach and Stream. Among populations, the differences were slightly significant. Only at temperatures above +10°C, *P. antarctica* pop. Beach presented a slightly higher assimilation rate than *P. antarctica* pop. Stream.

© 2024 The Authors.


1365313x, 0, Downloaded from https://onlinelibrary.wiley.com/doi/10.1111/tpj.16742 by Institution Nac De Investig Tec Agra, Wiley Online Library on [24/05/2024]. See the Terms and Conditions (https://onlinelibrary.wiley.com/terms-and-conditions) on Wiley Online Library for rules of use; OA articles are governed by the applicable Creative Commons License

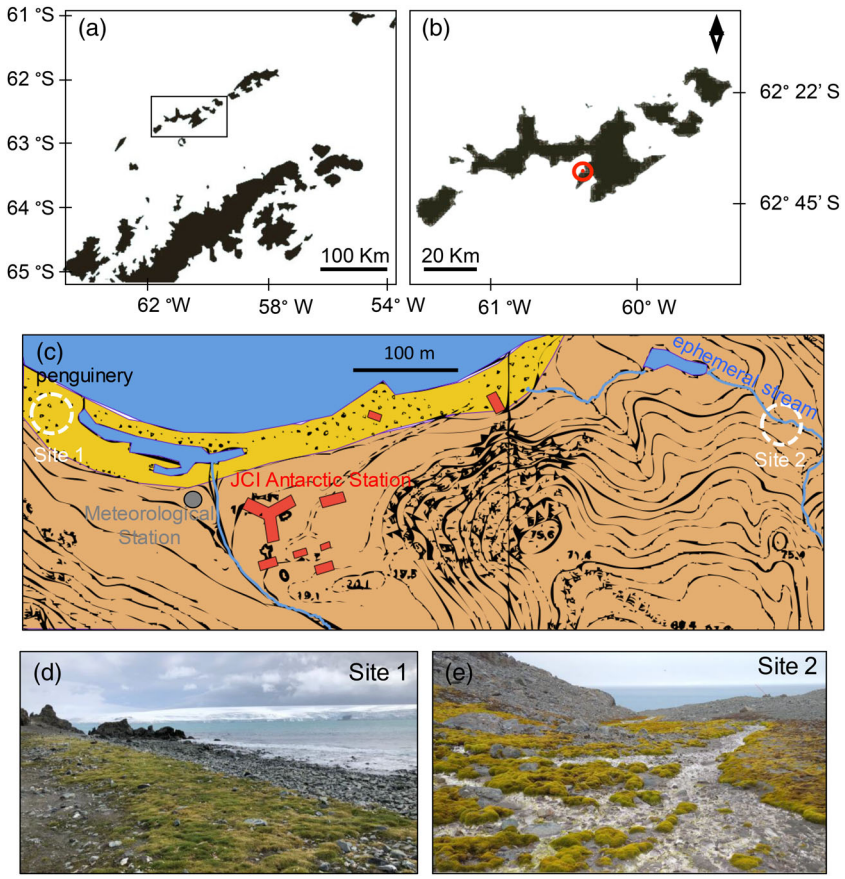



**Figure 1.** An overview of the two field sites of study.
(a) Livingston Island (highlighted in the Center of the square) in the South Shetland Islands at the NW of the Antarctic Peninsula.
(b) Location of the Spanish Antarctic Research Station Juan Carlos I (BAE JCI), in Livingston Island, highlighted with a red dot.
(c) Detail of the vicinities of the BAE JCI, showing the two sites of study: *Site 1*: located in a coastal area close to a penguinery of Gentoo penguin, *Site 2*: ephemeral fresh water stream, located several hundred metres aside from the Station at approximately 30 m a.s.l. The picture also shows the buildings of the BAE JCI (in red) and the meteorological station (grey dot).
(d, e) Show the general aspect of *Sites 1* and *2*, respectively.

Based on the overall maximum values of $A_{N500}$ around +20°C, the effect of $CO_2$ concentration was analysed in both populations at this temperature. Given that ETR/$A_N$ values were within the ratio values for non-stressed plants (Perera-Castro & Flexas, 2023) we were able to estimate $C_c$ and $g_{nsd}$ according to Harley et al. (1992) and therefore we built $A_{N500}$–$C_c$ curves (Figure 4C). In both cases, $A_{N500}$ increased with $CO_2$ and stabilised around 600 μmol mol$^{-1}$. However, *P. antarctica* pop. Beach presented significantly higher values of $A_{N500}$. These results were also perceptible on the photosynthetic parameters derived from the curves (Table S1) where the electron transport rate (ETR) at saturating light ($J_{high}$) of *P. antarctica* pop. Beach was 40% higher than that of *P. antarctica* pop. Stream and the maximum rate of carboxylation ($V_{cmax}$) was also 30% higher in Beach population. Likewise, the calculated non-stomatal diffusion conductance ($g_{nsd}$) was 61% higher in Beach population than in Stream population (Table 1). Analysing the limitations to photosynthesis based on Grassi and Magnani (2005), we could quantify the impact of each limitation on photosynthesis. We detected that the biochemical limitation related to $V_{cmax}$ was responsible of 38% of the lower values of *P. antarctica* pop. Stream and the non-stomatal diffusional limitation was responsible of the other 62%.

Accordingly, ETRs were slightly but significantly higher in *P. antarctica* pop. Beach (Table 1), but as observed with carbon assimilation, temperature had a direct effect (Figure 5; Table S2). The lowest ETR values were obtained at +4°C, while the highest were observed at +20°C. Rapid light curves (RLCs) indicated that only at +4°C both populations presented a decrease in PSII efficiency and this happened even at low irradiances (around 200 μmol m$^{-2}$ s$^{-1}$ PPFD) (Figure 5A,B; Table S2). Different parameters were derived from RLC (Table S2). Among others, the ETR at 475 μmol m$^{-2}$ s$^{-1}$ PPFD was analysed, as the closest measured irradiance point to 500 μmol m$^{-2}$ s$^{-1}$ PPFD

© 2024 The Authors.


1365313x, 0, Downloaded from https://onlinelibrary.wiley.com/doi/10.1111/tpj.16742 by Institution Nac De Investig Tec Agra, Wiley Online Library on [24/05/2024]. See the Terms and Conditions (https://onlinelibrary.wiley.com/terms-and-conditions) on Wiley Online Library for rules of use; OA articles are governed by the applicable Creative Commons License

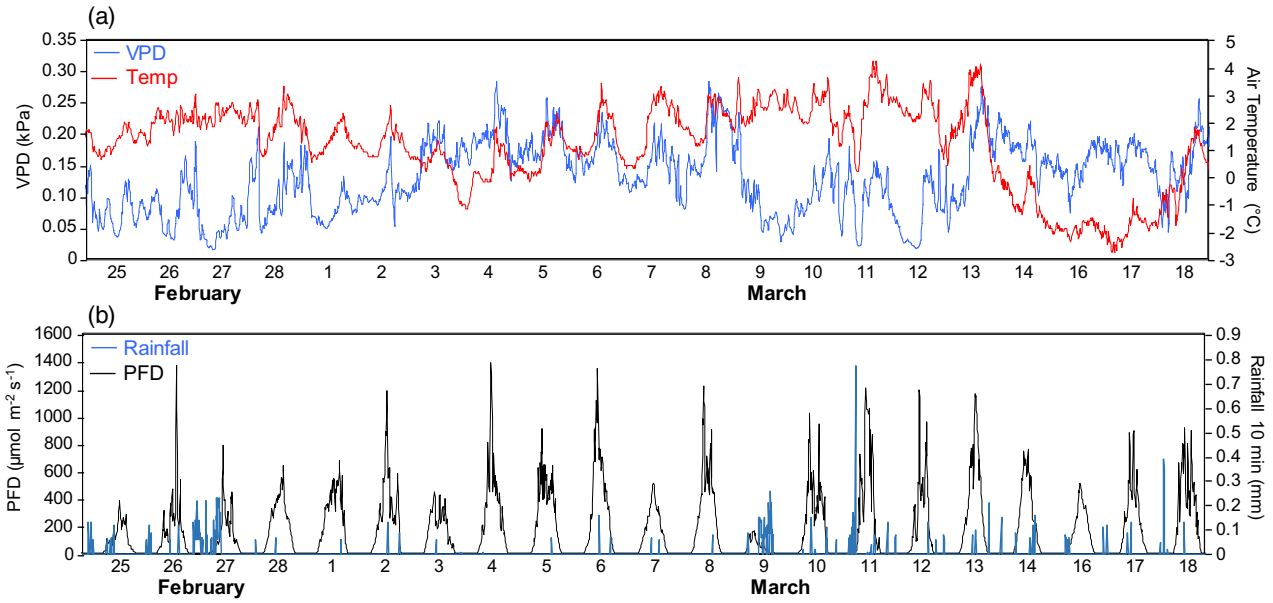



**Figure 2.** Meteorological conditions at the field site during the study period (24th February to 19th March 2022).
(a) VPD and air temperature.
(b) PFD and 10-min rainfall. PFD, photon flux density; VPD, vapour pressure deficit.

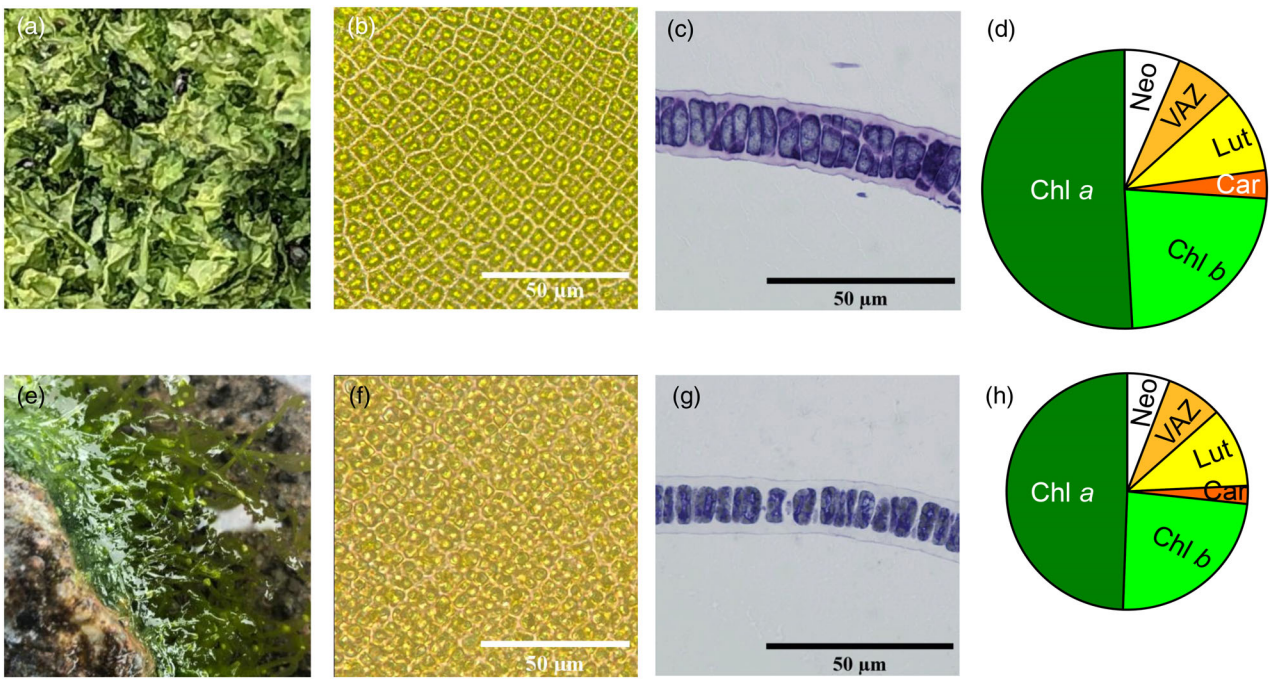



**Figure 3.** Morphology and photosynthetic pigment composition of *Prasiola antarctica* samples of both populations [(a–d) pop. Beach and (e–h) pop. Stream]. From left to right: (a, e) macroscopic view showing the foliose habit for pop. Beach and the filamentous habit for pop. Stream.
(b, f) Habit of the blade in surface view under the light microscopy, evidencing thickenings and areolae for pop. Beach samples.
(c, g) Cross-section of the thalli stained with toluidine blue.
(d, h) Pie charts of the main pigments composition.

(Figure 5C,D). Temperature rise had a significant increase in ETR in both populations, but the highest values were reached by *P. antarctica* pop. Beach at +20°C. Moreover, the correlation between temperature increase and $ETR_{475}$ or $ETR_{max}$ were analysed and for both parameters, the relation was linear until +20°C (Figure S2). The comparison between

© 2024 The Authors.


1365313x, 0, Downloaded from https://onlinelibrary.wiley.com/doi/10.1111/tpj.16742 by Institution Nac De Investig Tec Agra, Wiley Online Library on [24/05/2024]. See the Terms and Conditions (https://onlinelibrary.wiley.com/terms-and-conditions) on Wiley Online Library for rules of use; OA articles are governed by the applicable Creative Commons License

| Parameter | *P. antarctica* pop. Beach | *P. antarctica* pop. Stream | Units |
|---|---|---|---|
| Cell height | 11.83 ± 0.22a | 9.09 ± 0.22b | µm |
| Cell width | 4.32 ± 0.21a | 3.63 ± 0.21a | µm |
| Wall thickness | 1.84 ± 0.16b | 2.82 ± 0.16a | µm |
| Blade thickness | 15.51 ± 0.25a | 14.74 ± 0.25b | µm |
| Wall percentage | 32.04 ± 0.77b | 42.01 ± 0.77a | % |
| $A_{N500}$ | 0.64 ± 0.09a | 0.4 ± 0.05a | µmol $CO_2$ $m^{-2}$ $s^{-1}$ |
| $ETR_{max}$ | 6.09 ± 0.78b | 8.39 ± 0.28a | µmol $e^-$ $m^{-2}$ $s^{-1}$ |
| $g_{nsd}$ | 20.03 ± 2.19a | 12.41 ± 1.66b | mmol $CO_2$ $m^{-2}$ $s^{-1}$ |
| Ice nucleation temperature | −2.94 ± 0.45a | −2.15 ± 0.12a | °C |

**Table 1** Selected descriptive traits of both populations of *Prasiola antarctica* thalli

Carbon assimilation at 500 photosynthetic photon flux density (PPFD) ($A_{N500}$) and maximum electron transport rate ($ETR_{max}$) were measured at 4°C. Non-stomatal diffusional conductance ($g_{nsd}$) was measured at 20°C. Data are mean ± SE ($n$ = 4). Different letters represent significant differences between populations ($P$ < 0.05).

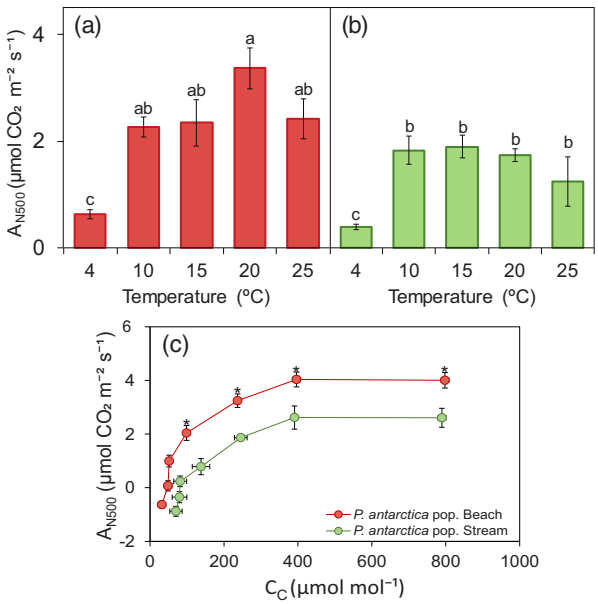



**Figure 4.** Effect of temperature on carbon assimilation.
Carbon assimilation in *Prasiola antarctica* pop. Beach [(A), red] and *P. antarctica* pop. Stream [(B), green] at different temperatures measured at 500 PPFD ($A_{N500}$).
(C) $A_{N500}$–$C_c$ curves of *P. antarctica* pop. Beach (red) and *P. antarctica* pop. Stream (green) measured at 500 photosynthetic photon flux density (PPFD) and 20°C. Data are mean ± SE ($n$ = 4). Letters represent significant differences between populations and different temperatures in (A, B) ($P$ < 0.05) and asterisks represent statistically significant differences between populations in (C) ($P$ < 0.05).

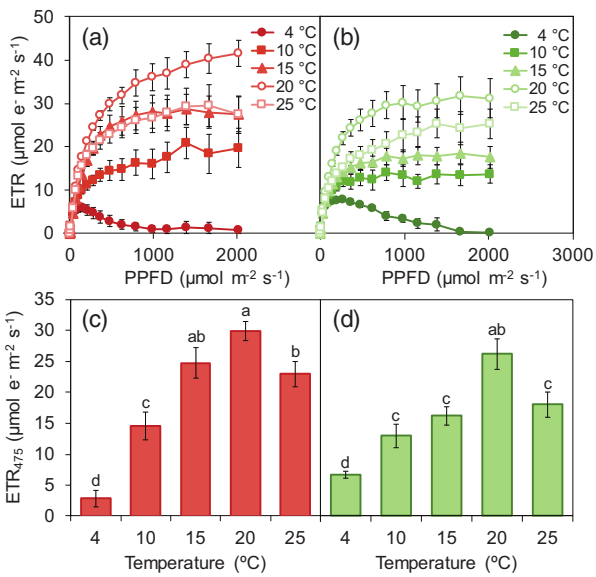



**Figure 5.** Effect of temperature on the electron transport rate (ETR).
(A, B) ETR curves of *Prasiola antarctica* pop. Beach (red) and *P. antarctica* pop. Stream (green) at different temperatures.
(C, D) ETR at 475 photosynthetic photon flux density (PPFD) obtained from the ETR curves of *P. antarctica* pop. Beach (red) and *P. antarctica* pop. Stream (green) at different temperatures. Data represent mean ± SE ($n$ = 4–5). Different letters represent statistically significant differences between populations and temperatures ($P$ < 0.05).

populations showed that only in $ETR_{max}$ the response to temperature was different, presenting *P. antarctica* pop. Beach a higher tendency of increase.

### Stress tolerance

The response of both populations to desiccation and freezing was assessed in the laboratory of the BAE JCI (Figure 6). Both populations were tolerant to the desiccation treatments, as shown in the recovery of their initial values of the maximal photochemical efficiency of PSII ($F_v/F_m$) (Figure 6A,B). Only a significant difference was observed between populations at 5% relative humidity (RH), where *P. antarctica* pop. Stream was slightly less tolerant than *P. antarctica* pop. Beach. Water content measurements showed that both populations reached similar values of around or less than 0.2 g $H_2O$ $g^{-1}$ DW in all the

© 2024 The Authors.


1365313x, 0, Downloaded from https://onlinelibrary.wiley.com/doi/10.1111/tpj.16742 by Institution Nac De Investig Tec Agra, Wiley Online Library on [24/05/2024]. See the Terms and Conditions (https://onlinelibrary.wiley.com/terms-and-conditions) on Wiley Online Library for rules of use; OA articles are governed by the applicable Creative Commons License

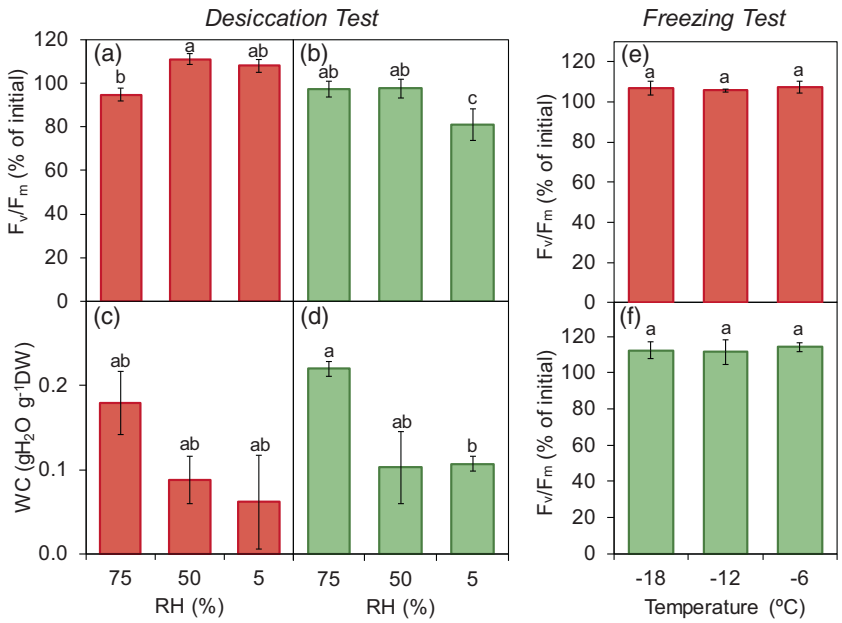



**Figure 6.** Tolerance of *P. antarctica* thalli to controlled desiccation and freezing.
(A, B) Recovery of $F_v/F_m$ after 48 h of desiccation treatment under different relative humidities (RH) and following rehydration in darkness at 20°C of *Prasiola antarctica* pop. Beach (red) and *P. antarctica* pop. Stream (green).
(C, D) Water content (WC) after desiccation treatment of *P. antarctica* pop. Beach (red) and *P. antarctica* pop. Stream (green).
(E, F) Recovery of $F_v/F_m$ after freezing treatment at different temperatures of *P. antarctica* pop. Beach (red) and *P. antarctica* pop. Stream (green). Data represent mean ± SE ($n = 3$). Letters indicate significant differences between populations and treatment levels ($P < 0.05$).

RH levels (Figure 6C,D). Likewise, freezing treatments indicated that both populations were able to recover from below zero temperatures in a short period of time, at least until −18°C (Figure 6E,F). In this case, no significant differences were detected among populations. Accordingly, the ice nucleation temperature was above −3°C for both populations, also without significant differences between them (Table 1).

On the basis of the proven tolerance, we wanted to deepen in the alterations that occurred in both populations during desiccation. For this purpose, the two populations were subjected to a moderate desiccation treatment at 50% RH and +4°C for 40 h (Figure 7). Water loss of both populations was monitored during desiccation. The loss of absolute water content and relative water content (RWC) was similar in between them. Even if not significant, it is worth noting that *P. antarctica* pop. Stream presented higher absolute water content values and more pronounced RWC loss than *P. antarctica* pop. Beach (Figure 7a,b). The maximal photochemical efficiency of PSII ($F_v/F_m$), estimated through Chl *a* fluorescence measurements, progressively decreased during desiccation, being significantly different between both populations only 14 h after the beginning of the treatment (Figure 7c,d). Deeper analyses of the data [e.g. correlation between $F_v/F_m$ and RWC (Figure S3)] showed that $F_v/F_m$ started to decrease when the RWC was around 50% in the two populations.

### Photoprotection and stress

Alterations in the content of main photoprotective molecules in response to the controlled desiccation treatment were also analysed by comparison of hydrated and desiccated samples (Figure 8). The xanthophyll cycle carotenoids violaxanthin (V), antheraxanthin (A) and zeaxanthin (Z) were analysed. The VAZ/Chl *a* + *b* ratio was rather high (≥80 mmol mol$^{-1}$), but very similar between populations and was not significantly altered during desiccation (Figure 8A). This was also the case for the total content of carotenoids (Car/Chl *a* + *b*, Figure 8C). In contrast, both AZ/VAZ ratio and α-tocopherol (α-Toc/Chl *a* + *b*) were significantly different (Figure 8B,D; Table S3). During desiccation, AZ/VAZ only increased significantly in *P. antarctica* pop. Stream, indicating differences among populations but also in response to the treatment. The α-Toc/Chl *a* + *b* ratio did not change with the treatment, but *P. antarctica* pop. Beach contained three times higher levels than *P. antarctica* pop. Stream (Figure 8D).

### Lipids and stress

Polar lipid content (phospholipids and glycerolipids) was the same in hydrated thalli of both populations (around 37 nmol g$^{-1}$ DW) and was not affected by desiccation (Table 2). Major components of the lipidome were DGDG and MGDG among GLs (together representing 74–83% of

© 2024 The Authors.


1365313x, 0, Downloaded from https://onlinelibrary.wiley.com/doi/10.1111/tpj.16742 by Institution Nac De Investig Tec Agra, Wiley Online Library on [24/05/2024]. See the Terms and Conditions (https://onlinelibrary.wiley.com/terms-and-conditions) on Wiley Online Library for rules of use; OA articles are governed by the applicable Creative Commons License

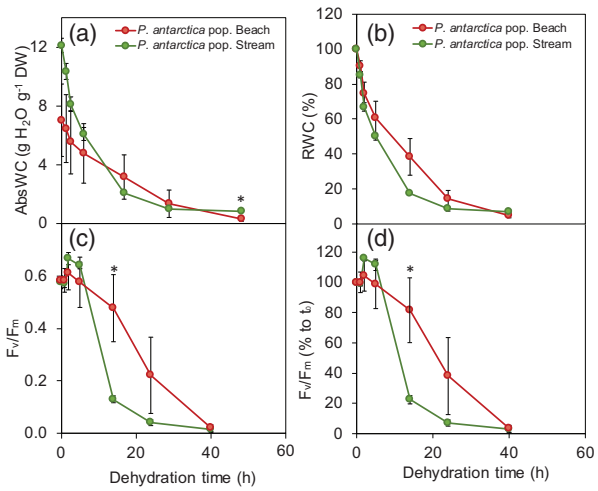



**Figure 7.** Water relations and kinetics of $F_v/F_m$ of *Prasiola antarctica* populations during controlled desiccation.
Changes in absolute water content (a), relative water content (RWC) (b), $F_v/F_m$ (c) and percentage of $F_v/F_m$ (d) during desiccation treatment at 50% relative humidity (RH) and 4°C of *P. antarctica* pop. Beach (red) and *P. antarctica* pop. Stream (green). Data are mean ± SE ($n$ = 4). Asterisks indicate statistically significant differences between populations ($P$ < 0.05).

the GL pool) and phosphatidylcholine (PC) and phosphatidylinositol (PI) among phospholipids (together representing 62–68% of the phospholipid pool), with a lower proportion of trigalactosyldiacylglycerol (TGDG), phosphatidylglycerol (PG), phosphatidylethanolamine (PE) and phosphatidylserine (PS) and a negligible amount of tetragalactosyldiacylglycerol (TeGDG). Desiccation only induced changes in *P. antarctica* pop. Beach among the major polar lipids (MGDG, PC and PE increased).

The most abundant molecular species among GLs (Figure 9) were those containing 34 carbons, in particular, those with six double bonds (34:6), which accounted for 52 and 62% of the total GL pool in the Beach and Stream population, respectively. This pattern was the same irrespective of the number of galactose residues of the polar head, except in the case of TeGDG whose most abundant molecular species was (42:5). For the case of phospholipids (Figure S4) the most abundant species contained 34 carbons (34:2) for PG and PI, 38 carbons (38:6) for PC and 40 carbons (40:7) for PE. Fatty acid unsaturation did not differ much between both populations and it was higher in GLs than in phospholipids, with desaturation increasing in the

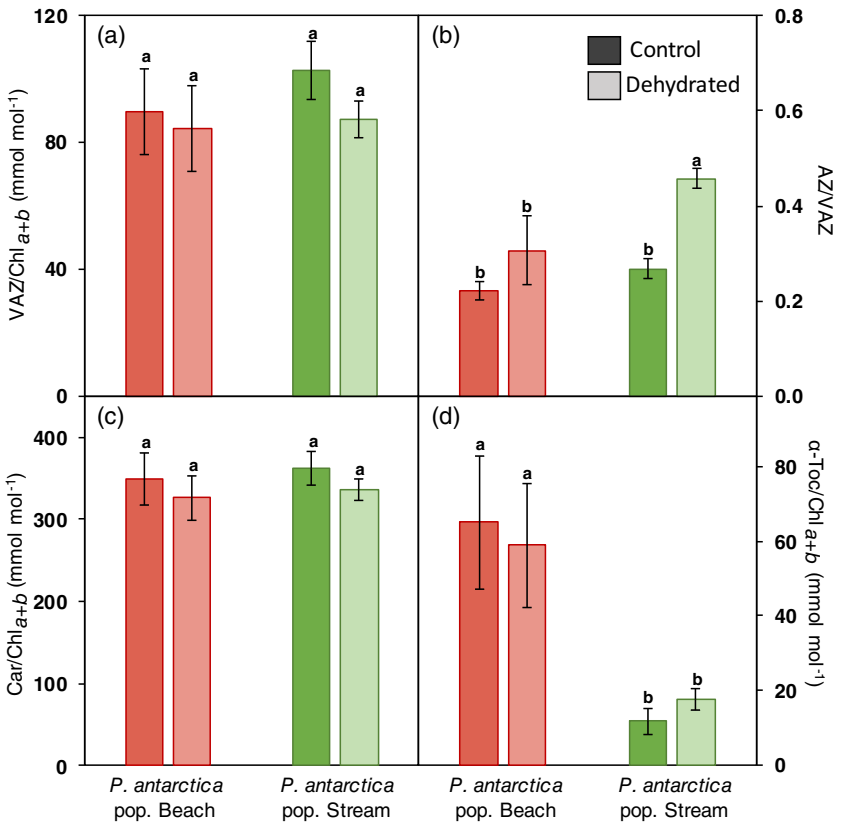



**Figure 8.** Photoprotection mechanisms of *Prasiola antarctica* thalli to controlled desiccation in pop. Beach (red) and pop. Stream (green).
Changes in VAZ/Chl (A), AZ/VAZ (B), Car/Chl (C) and α-Toc/Chl (D) during desiccation treatment at 50% relative humidity (RH) and 4°C (light colour). Data are mean ± SE ($n$ = 5). Letters indicate statistically significant differences between populations and treatment ($P$ < 0.05).

© 2024 The Authors.


1365313x, 0, Downloaded from https://onlinelibrary.wiley.com/doi/10.1111/tpj.16742 by Institution Nac De Investig Tec Agra, Wiley Online Library on [24/05/2024]. See the Terms and Conditions (https://onlinelibrary.wiley.com/terms-and-conditions) on Wiley Online Library for rules of use; OA articles are governed by the applicable Creative Commons License

**Table 2** Main polar lipid composition of *Prasiola antarctica* populations under controlled desiccation treatment (nmol $mg^{-1}DW$)

| | *P. antarctica* pop. Beach | | *P. antarctica* pop. Stream | | Two-way ANOVA | | |
|---|---|---|---|---|---|---|---|
| Polar lipid | Control | Dehydrated | Control | Dehydrated | Population | Treatment | Interaction |
| DGDG | 5.47 ± 0.63a | 5.69 ± 0.55a | 4.55 ± 0.27a | 5.47 ± 0.52a | 0.28 | 0.28 | 0.51 |
| MGDG | 3.73 ± 1.19b | 9.45 ± 1.27a | 5.13 ± 0.57b | 5.44 ± 1.14b | 0.25 | **0.01** | **0.02** |
| TGDG | 3.18 ± 0.10a | 2.94 ± 0.24ab | 2.29 ± 0.08c | 2.60 ± 0.14bc | ***P* < 0.01** | 0.85 | 0.09 |
| TeGDG | 0.03 ± 0.02b | 0.07 ± 0.01b | 0.13 ± 0.02a | 0.05 ± 0.01b | ***P* < 0.01** | 0.15 | ***P* < 0.01** |
| PG | 1.95 ± 0.19a | 1.82 ± 0.32a | 1.37 ± 0.07a | 1.46 ± 0.16a | **0.04** | 0.93 | 0.59 |
| PC | 4.15 ± 0.67b | 9.42 ± 1.38a | 3.85 ± 0.19b | 3.53 ± 1.58b | **0.01** | **0.04** | **0.02** |
| PE | 2.34 ± 0.39b | 4.29 ± 0.41a | 2.57 ± 0.12b | 3.16 ± 0.86ab | 0.4 | **0.03** | 0.21 |
| PI | 6.16 ± 0.24a | 5.54 ± 0.26a | 5.61 ± 0.23a | 6.05 ± 0.34a | 0.93 | 0.74 | 0.07 |
| PS | 0.99 ± 0.07bc | 0.94 ± 0.05c | 1.20 ± 0.10ab | 1.26 ± 0.10a | ***P* < 0.01** | 0.94 | 0.46 |
| PA | 3.99 ± 0.48ab | 1.41 ± 0.47b | 5.67 ± 0.50a | 5.10 ± 1.58a | ***P* < 0.01** | 0.1 | 0.28 |
| LPG | 0.23 ± 0.03a | 0.03 ± 0.02c | 0.18 ± 0.01ab | 0.10 ± 0.04bc | 0.8 | ***P* < 0.01** | **0.04** |
| LPC | 3.09 ± 0.31a | 0.90 ± 0.12c | 2.45 ± 0.14ab | 1.70 ± 0.44bc | 0.79 | ***P* < 0.01** | **0.02** |
| LPE | 1.12 ± 0.04ab | 0.44 ± 0.07c | 1.33 ± 0.08a | 0.90 ± 0.15b | ***P* < 0.01** | ***P* < 0.01** | 0.19 |
| DGTS | 0.00 ± 0.00ab | 0.01 ± 0.00a | 0.00 ± 0.00ab | 0.00 ± 0.00b | **0.03** | 0.76 | 0.1 |
| MGTS | 0.43 ± 0.10a | 0.06 ± 0.02b | 0.20 ± 0.04b | 0.06 ± 0.02b | 0.05 | ***P* < 0.01** | 0.05 |
| Total | 36.86 ± 2.63a | 43.01 ± 3.13a | 36.53 ± 1.13a | 36.88 ± 1.95a | 0.184 | 0.183 | 0.235 |

Desiccation treatment was conducted at 50% relative humidity (RH) and +4°C. Data are mean ± SE ($n = 5$). Letters indicate significant differences between populations and treatment ($P < 0.05$). The results of the two-way analysis of variances for the effect of population and treatment for each lipid are indicated on the right columns of the table ($P < 0.05$). *P*-values are indicated in bold when significant at $P < 0.05$.
DGDG, digalactosyldiacylglycerol; DGTS, diacylglyceryltrimethylhomoserine; LPC, lysophosphatidylcholine; LPE, lysophosphatidylethanolamine; LPG, lysophosphatidylglycerol; MGDG, monogalactosyldiacylglycerol; MGTS, monoacylglyceryltrimethylhomoserine; PA, phospatidic acid; PC, phosphatidylcholine; PE, phosphatidylethanolamine; PG, phosphatidylglycerol; PI, phosphatidylinositol; PS, phosphatidylserine; TeGDG, tetragalactosyldiacylglycerol; TGDG, trigalactosyldiacylglycerol.

order PI–PG–PS–PC–PE–TGDG–MGDG–DGDG (Figure S5). Desiccation induced a further increase of unsaturation in phospholipids, more noticeably in *P. antarctica* pop. Beach. The number of insaturations in the fatty acids of GLs was not affected by desiccation, being its unsaturation index close to a theoretical maximum of 300. Desiccation did not induce a significant rise in cylindrical GLs (DGDG, TGDG and TeGDG), which constitutively represented a high proportion of the total lipids in both populations (Figure 10).

## DISCUSSION

### Thriving in harsh environments requires thylakoid stability in *P. antarctica*

Antarctica is the coldest continent on Earth and the only one dominated by non-vascular vegetation (Ochyra et al., 2008; Øvstedal & Lewis Smith, 2001; Peat et al., 2007; Robinson et al., 2003). It is essentially a cold desert with extreme conditions that make it difficult for terrestrial photosynthetic organisms to thrive. The availability of crucial environmental factors within a range suitable for growth is greatly limited. These are mainly irradiance (which is seasonally restricted and decreases with increasing latitude), temperature and liquid water (Robinson et al., 2003). Additionally, more than 90% of the land is covered by permanent ice. This restricts the distribution of the vegetation to the 0.44% of ice-free surface, which is additionally the space where humans exert most of their disturbance (Brooks et al., 2019). Despite these challenges, Antarctica still sustains a significant bulk of photosynthetic organisms and their biochemical mechanisms and capacity to acclimate to a changing environment are largely understudied (Colesie et al., 2023). Understanding their morphological and physiological adaptations to thrive in such a harsh environment is essential for making more accurate predictions about the effects of climate change on vegetation (Colesie et al., 2023) and could set the basis to decipher key mechanisms for improving the photosynthetic capabilities of model organisms too (Fernández-Marín, Gulías, et al., 2020; Levin et al., 2021).

The species within the genus *Prasiola* represent some of the most outstanding photosynthetic organisms of Antarctica. Overall, they represent one of the primary food sources and habitat of Antarctica in many terrestrial and supralittoral ecosystems (Davis, 1981; Lukashanets et al., 2022). They dominate vegetation communities in the surroundings of bird colonies standing relatively high soil contents of nitrogen and phosphorus (Abakumov et al., 2021; Durán et al., 2021) and also serve as habitat for dense populations of invertebrates (Lukashanets et al., 2022). Specifically, our results evidence the exceptional capabilities of *P. antarctica*, which is able to succeed in very contrasting micro environments such as terrestrial supralittoral belt and fresh-water ephemeral streams. In

© 2024 The Authors.


1365313x, 0, Downloaded from https://onlinelibrary.wiley.com/doi/10.1111/tpj.16742 by Institution Nac De Investig Tec Agra, Wiley Online Library on [24/05/2024]. See the Terms and Conditions (https://onlinelibrary.wiley.com/terms-and-conditions) on Wiley Online Library for rules of use; OA articles are governed by the applicable Creative Commons License

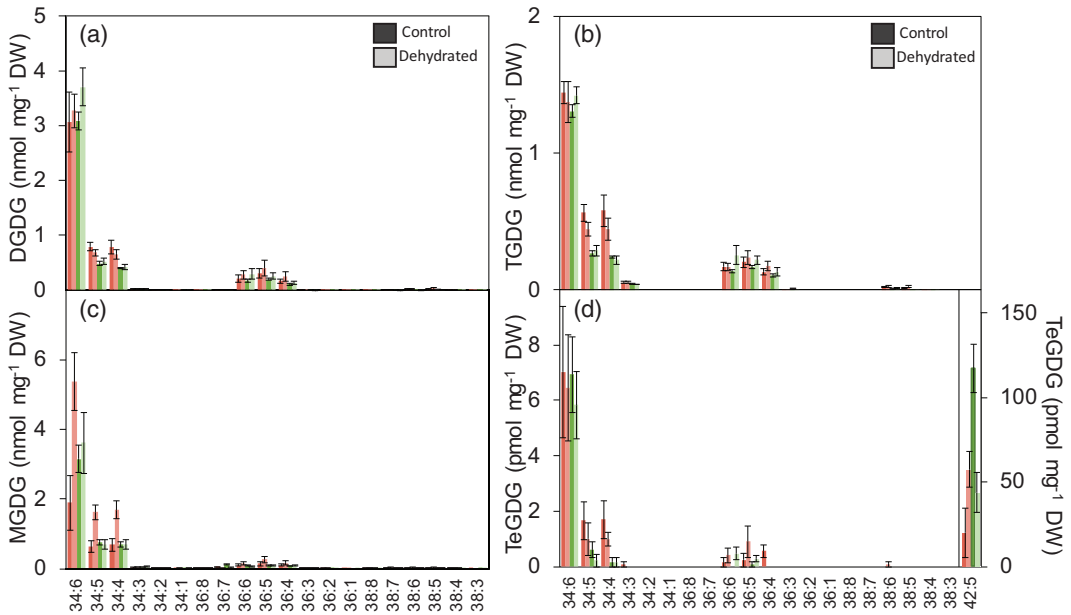



**Figure 9.** Molecular species composition of galactolipids in *Prasiola antarctica* populations under controlled desiccation treatment.
Differences in molecular species of DGDG (a), TGDG (b), MGDG (c) and TeGDG (d) analysed in *P. antarctica* pop. Beach (red) and *P. antarctica* pop. Stream (green) before (bright colour) and after (light colour) desiccation treatment at 50% relative humidity (RH) and 4°C. Data represent mean ± SE ($n = 5$). DGDG, digalactosyldiacylglycerol; MGDG, monogalactosyldiacylglycerol; TeGDG, tetragalactosyldiacylglycerol; TGDG, trigalactosyldiacylglycerol.

the light of our results, *P. antarctica* is remarkably tolerant to desiccation and freezing stress, e.g. can survive a drop of water content down to 0.1 g $H_2O$ $g^{-1}$ DW and can tolerate, in the hydrated state, temperatures down to −18°C (Figure 6).

The capacity to withstand freezing temperatures down <−18°C is shared with other Antarctic species of the genus, such as *P. crispa* (Bacior et al., 2022; Becker, 1982; Fernández-Marín, López-Pozo, et al., 2019; Kosugi et al., 2010), but the molecular mechanism enabling it are not yet fully understood (Bacior et al., 2022). The accumulation of compatible and soluble osmolytes, such as proline, seems to be part of the biochemical mechanism enabling freezing tolerance in *P. crispa* (Jackson & Seppelt, 1995). However, some other important adaptations to thrive in extreme environments include the ability to maintain membrane stability (Fernández-Marín, Gulías, et al., 2020; Gasulla et al., 2019). Photosynthetic organisms respond to changes in environmental conditions by modifying the chemical composition of their membranes to optimise their functions including their direct interaction with photosynthetic complexes, a process known as lipid remodelling (Chng et al., 2021; Yoshihara & Kobayashi, 2022; Yu et al., 2021). This can be achieved by modification of the acyl chain (desaturation and/or length) or the polar head group. While the overall lipid composition of our populations of *P. antarctica* was similar to other algae species (Gasulla et al., 2016; Sato et al., 2003) the acyl chain composition differed markedly, with a much higher degree of unsaturation (34:6 was the dominant molecular species). The enhancement of fatty acid chain unsaturation in response to low temperatures is a process widely described (Welti et al., 2002) that contributes to the thermal adjustment of membrane fluidity (Ernst et al., 2016). High content of polyunsaturated fatty acids has also been reported for arctic populations of *P. crispa* with domination of 18:3 molecular species (Graeve et al., 2002). The degree of unsaturation was particularly high in the case of GLs of *P. antarctica*, with fatty acid unsaturation values close to the theoretical limit of 300 (Figure S5), which means that all acyl chains have three desaturations. TGDG, in particular, comprised a very high proportion (close to 100%) of polyunsaturated fatty acids (18:3, 18:2, 16:3, among others).

In response to freezing and desiccation, the proportion of cylinder-shaped lipids increases, with concomitant decrease of conic-shaped lipids, a process that decreases the risk of formation of non-bilayer membranes (Gasulla et al., 2019). This is typically reflected by an enhancement of the PC:PE or the DGDG:MGDG ratios (Yu et al., 2021). Thylakoid stability can be further enhanced by the presence of glycolipids with larger polar heads: TGDG and TeGDG, with three and four galactose residues, respectively. In *P. antarctica* the content of TGDG represented between 16 and 26% of total GL content, a ratio 5–10 times higher than that of other photosynthetic organisms, such as chlorophyte algae (Gasulla et al., 2016), which represents an exceptionally high constitutive content. Among

© 2024 The Authors.


1365313x, 0, Downloaded from https://onlinelibrary.wiley.com/doi/10.1111/tpj.16742 by Institution Nac De Investig Tec Agra, Wiley Online Library on [24/05/2024]. See the Terms and Conditions (https://onlinelibrary.wiley.com/terms-and-conditions) on Wiley Online Library for rules of use; OA articles are governed by the applicable Creative Commons License

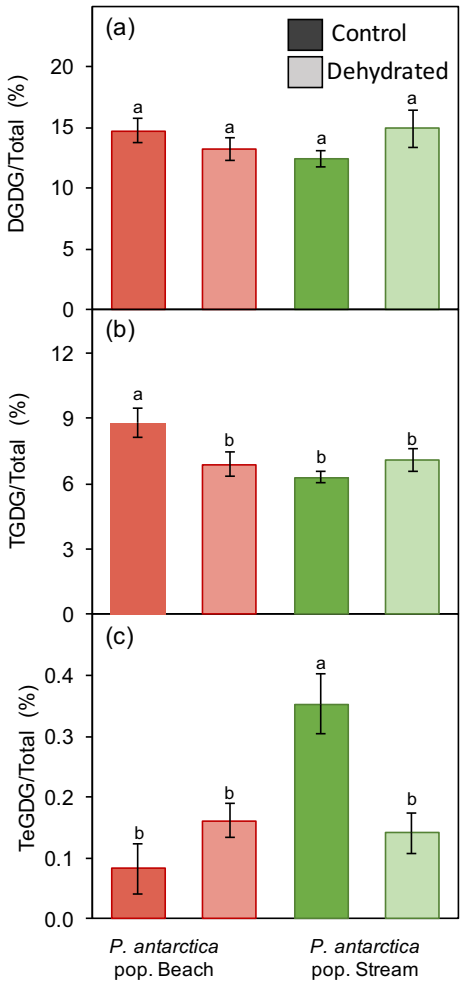



**Figure 10.** Percentage of oligogalactolipid composition of *Prasiola antarctica* populations under controlled desiccation treatment.
Changes in DGDG/Total (A), TGDG/Total (B) and TeGDG/Total (C) before (solid) and after the desiccation treatment conducted at 50% relative and 4°C (light colour) of *P. antarctica* pop. Beach (red) and *P. antarctica* pop. Stream (green). Data represent mean ± SE ($n = 5$). Letters indicate statistically significant differences between populations and treatment ($P < 0.05$). DGDG, digalactosyldiacylglycerol; TeGDG, tetragalactosyldiacylglycerol; TGDG, trigalactosyldiacylglycerol.

other phototrophs, a comparable proportion of TGDG has been described in some cold-water dinoflagellate species (Flaim et al., 2012; Leblond et al., 2010) and after freezing-acclimation in leaves of the cold-tolerant angiosperm *Boecheria stricta* (Arisz et al., 2018). Moreover, it is assumed that the presence of cylinder-shaped TGDG with large polar heads is necessary to stabilise thylakoids when water content drops (Chng et al., 2021). In that sense, the TGDG/DGDG ratio of 0.6 obtained in *P. antarctica* is higher than that found in other desiccation tolerant photosynthetic organisms: e.g. 0.05 in chlorophyllous fern spores (López-Pozo et al., 2019) or 0.1–0.2 in leaves of resurrection angiosperms (Fernández-Marín, Nadal, et al., 2020). Indeed, Gasulla et al. (2013) have shown that TGDG content also responds positively to desiccation stress in the resurrection plant *Craterostigma plantagineum*. In spite of the high responsiveness of TGDG to environmental stress in angiosperms, in *P. antarctica*, it was not affected by desiccation, being the constitutive content of TGDG high in hydrated thalli in both populations (Figure 10). Physical stability and protection of the thylakoid membranes is also reinforced by xanthophylls, such as antheraxanthin and, more importantly, zeaxanthin (Grudzinski et al., 2017; Havaux, 1998). The total pool size of xanthophyll cycle pigments (e.g. VAZ) is variable in response to cumulative demanding requirements (Esteban et al., 2015). So, the high VAZ/Chl repeatedly found in different species at high latitudes may indicate a pre-emptive protective stage of the photosynthetic membranes in these harsh environments where low temperature, intermittent water availability and irradiance converge (Fernández-Marín, Gago, et al., 2019; Fernández-Marín, López-Pozo, et al., 2019; García-Plazaola, López-Pozo, & Fernández-Marín, 2022). The elevated VAZ/Chl values obtained in *P. antarctica* are in agreement with previous reports at high latitudes, where most photosynthetic organisms are subjected to high thylakoid protection requirements. Altogether, these findings suggest that the harsh Antarctic conditions favour stability (higher TGDG:MGDG to avoid destabilisation and membrane fusion) in thylakoids membranes of *P. antarctica*, as well as more fluidity (high unsaturation values to favour the rate of electron transport chain redox reactions).

### Anatomy and photosynthesis in *P. antarctica*

At a higher cellular scale, the studied specimens of *P. antarctica* had a monostromatic thalli with a blade thickness and protoplast size similar to other *Prasiola* species (Holzinger et al., 2006; Richter et al., 2017) including *P. antarctica* (Jacob, Lehmann, et al., 1992), which was referred to as '*P. crispa* subsp. *Antarctica*' in bibliography prior to Moniz et al. (2012). Also cell wall thickness was comparable to previously analysed *Prasiola* spp. (around 2–3 μm) which is remarkably thicker than in other terrestrial algae, e.g. 0.1–0.3 μm in *Chlorella vulgaris*, *Coelastrella*, *Haematococcus pluvialis* and *Scenedesmus* (Spain & Funk, 2022). The thicker cell walls may be necessary for desiccation tolerance, to prevent tissue damage during dehydration (Nadal et al., 2021) and be related to their adaptations to the harsh environments of Antarctica. In turn, this could also be partly a reason behind the relatively low carbon assimilation rate obtained for *P. antarctica* at ambient temperature of +4°C (<1 μmol $CO_2$ $m^{-2}$ $s^{-1}$), since thick cell walls (but also its specific porosity and chemical composition) are generally related to lower assimilation values, due to $CO_2$ diffusional limitations (Flexas et al., 2021; Nadal et al., 2021). Indeed, the effect of the thicker cell walls was partially reflected in low non-stomatal conductance $g_{nsd}$ values. These values

© 2024 The Authors.


1365313x, 0, Downloaded from https://onlinelibrary.wiley.com/doi/10.1111/tpj.16742 by Institution Nac De Investig Tec Agra, Wiley Online Library on [24/05/2024]. See the Terms and Conditions (https://onlinelibrary.wiley.com/terms-and-conditions) on Wiley Online Library for rules of use; OA articles are governed by the applicable Creative Commons License

are similar to the ones obtained in other non-vascular plants in Antarctica (Carriquí et al., 2019; Perera-Castro et al., 2020; Roig-Oliver et al., 2021). However, we could not compare to other algae, since to the best of our knowledge, this is the first time that a diffusion conductance is calculated in algae.

Temperature is another factor greatly affecting the efficiency of carbon assimilation. Photopsychrotolerant organisms are able to acclimate and live at low temperatures (from 0 to +5°C), but present higher growth rates at elevated temperatures (≥+20°C) (Hüner et al., 2022; Morita, 1975). Thus, in the light of the results obtained, *P. antarctica* is a photopsychrotolerant species. Optimal high temperatures for net carbon assimilation (between +15 and +25°C) are rather frequent among terrestrial photosynthetic organisms in Antarctica including bryophytes (Perera-Castro et al., 2020), lichens (Kappen et al., 1998) and other species of *Prasiola* too (Kosugi et al., 2010). Even when air temperatures are rarely above +10°C in the study site [i.e. recent record for Livingston Island was +12.6°C during the 6–11 February 2022 heatwave that affected Maritime Antarctica (González-Herrero et al., 2022)], tissue temperature can rise several degrees above the air temperature as a consequence of incident irradiance (Perera-Castro et al., 2020, 2021). In our study, optimal temperature obtained for the net carbon assimilation of *P. antarctica* fell within the range of +10 to +25°C. Interestingly, in a global warming context, *P. antarctica* may thus find advantages with a significant rise in its growth capacity. Nonetheless, this temperature-dependent increase was different between ETR and $A_{N500}$ (Figures 3 and 4). This uncoupling may indicate an important photoprotection demand for *P. antarctica* and even so, some energy can be risky diverted to $O_2$ as electron acceptor, which must be accompanied by an accumulation of antioxidants to mitigate the oxidative damage (Foyer et al., 1994). Although less probable, an effect of temperature on the absorbance of photosystems as a potential reason behind this uncoupling cannot be totally rejected. These temperature-dependent changes do not significantly vary in Antarctic bryophytes (Perera-Castro et al., 2020), but have not been specifically tested for *Prasiola* yet.

In cold environments, there can be an imbalance between the absorption of light and the capacity of photosynthesis to use that energy (Ort, 2001). To obtain a balance, also called photostasis, the fast first photobiophysical processes of light absorption and electron transfer must be coupled with the much slower second process of photochemistry associated with the electron transport chain redox reactions and with the soluble enzymes of the Calvin-Benson-Bassham Cycle (Hüner et al., 2022). The first process is temperature independent, whereas the second one is temperature dependent. Therefore, one of the main challenges in polar regions for photoautotrophic organisms is to obtain a balance between the absorbed photons and transformed energy under extreme environmental conditions (Huner et al., 1998). To be able to withstand these conditions the photoautotrophs show various adaptations. On one hand, the observed high degree of unsaturation in the membrane lipids implies a more fluid membrane that could increase the rate of the electron transport chain redox reactions (Ernst et al., 2016; Welti et al., 2002). On the other hand, one of the mechanism to dissipate the excess of energy is through non-photochemical quenching which could be related to the high values detected of VAZ/Chl, around 90–100 mmol $mol^{-1}$, that fall within the upper limit of the expected range for terrestrial photosynthetic eukaryotes (Esteban et al., 2015). This high ratio is in agreement with data found for other Antarctic tundra species (García-Plazaola, López-Pozo, & Fernández-Marín, 2022). Even though, this was not enough to prevent a reduction on the ETR at the coldest temperature measured (as a consequence of down regulation of PSII efficiency), that already decreased at PPFD higher than 150 μmol $m^{-2}$ $s^{-1}$ in Stream population and 250 μmol $m^{-2}$ $s^{-1}$ in Beach population. At higher temperatures, electron source and sink reached photostasis, therefore, no down-regulation of PSII efficiency was detected.

### The trick to succeed: anatomical versus physiological plasticity in *P. antarctica*

The studied populations of *P. antarctica* live in different habitats that present distinct physico-chemical abiotic stressors. In Site 1, *P. antarctica* shows a terrestrial habit and is exposed to limited water availability, depending only on rain water and/or by a sporadic flood from the nearby stream and it is also exposed to direct sunlight that can increase the thalli temperature, as has been demonstrated to occur in other Antarctic species (Ohtani et al., 1990; Perera-Castro et al., 2020). Moreover, in this supralittoral habitat the proximity to sea water can result in exposition to salt spray (Jacob, Lehmann, et al., 1992). In Site 2, *P. antarctica* is submerged in a glacial water stream until summer end, when the stream flow disappears and the thalli emerges. Therefore, this population lives in a colder and more stable environment in terms of water availability and temperature. This population has probably less access to nutrients and is attached to rocks under the stress of the stream flow. Interestingly, previous studies have shown that *P. antarctica* has the capacity to grow under different salinities (Jacob et al., 1991). This adaptability to salinity is represented in our study by the selected populations and their different locations.

The two studied populations displayed varying morphologies at macroscopic and microscopic scale. Thalli architecture in pop. Stream was flattish and the width of each frond was thinner than pop. Beach, where the thalli was folded and tended to grow more stacked (Figure 3).

© 2024 The Authors.


1365313x, 0, Downloaded from https://onlinelibrary.wiley.com/doi/10.1111/tpj.16742 by Institution Nac De Investig Tec Agra, Wiley Online Library on [24/05/2024]. See the Terms and Conditions (https://onlinelibrary.wiley.com/terms-and-conditions) on Wiley Online Library for rules of use; OA articles are governed by the applicable Creative Commons License

These macroscopic changes were also detected by (Jacob, Lehmann, et al., 1992) when *P. antarctica* was grown in freshwater or seawater under controlled conditions. At a microscopic scale, cells were organised in groups of four and had similar width (around 4 μm), but in the case of pop. Stream the cells were more stacked. Biggest difference was found on the thickness and proportion of the cell wall (Table 1). The stream population had thicker cell walls (around 1 μm thicker). This higher thickness could be related to an adaptive response to hyposaline conditions to prevent the water influx occurring during osmoregulation (Jacob et al., 1991), or it could be an adaptation to reduce the mechanical damage related to current velocity of the stream flow. Remarkable morphological differences among populations occurring in ecologically contrasting habitats have also been reported for other *Prasiola* species. As an example, arctic populations of *P. crispa* are morphologically different in response to the proximity to bird colonies and the consequent differences on fertilisation (Richter et al., 2017), while *P. mexicana* shows a wide range of habitats and morphometric variations in mexican streams related to current velocity and irradiance (Ramírez et al., 2007).

Aside from morphological differences, photosynthetic performance in both populations was also different. Overall, pop. Beach showed significantly higher values than pop. Stream. The optimal temperature was slightly shifted towards higher values in pop. Beach (+20°C). This population also showed the highest rates of $A_N$, $J_{high}$ and $V_{cmax}$. Indeed, the analysis of the photosynthetic limitations showed that in Stream population the metabolic limitation (related to $V_{cmax}$) represented 32% of the difference. This limitation could be associated with the morphology of the thalli, where the pop. Beach has a greater proportion of protoplast and therefore, more photosynthetic active tissue. This can be also observed in a higher quantity of Chl in pop. Beach than in pop. Stream: 4.2 ± 0.3 versus 3.1 ± 0.5 Chl $a + b$ μmol $g^{-1}$ DW, respectively. These characteristics could lead to the idea that Beach population is behaving like 'sun-acclimated' individuals, comparing to the more shade-adapted individuals of Stream population. This idea is partially sustained by the values of Chl *a*/*b*, which presents slight difference among populations ($P = 0.096$). However, as there is no measured accumulated irradiance data available we can not conclude that Beach population presented a more 'sun-acclimated' character. Furthermore, a higher $V_{cmax}$ is usually related to a higher Rubisco content (Walker et al., 2014). Rubisco is the main N component, and therefore, the higher $V_{cmax}$ in *P. antarctica* pop. Beach than in pop. Stream could also be associated with the higher nutrient availability nearby the penguin colony. Because of this, it would be reasonable to expect a higher Rubisco content in the Beach population than in the Stream one. Another possible explanation for the differences in the photosynthetic performance between populations are the limitations of the diffusion of $CO_2$. Indeed, diffusional limitation represented 68% of the difference in photosynthesis in Stream population of the above-mentioned analysis of photosynthetic limitations. We did detect lower $g_{nsd}$ values in Stream population than in Beach population that indicate a lower ability for $CO_2$ diffusion through the wall. As a matter of fact, Stream population presented higher cell wall thickness than Beach population. Roig-Oliver et al. (2021) demonstrated in Antarctic mosses that thicker cell walls were related to lower assimilation rates, with relevance also of a different composition of the cell walls. This occurs because the combination of cell wall thickness and biochemical composition affects $CO_2$ diffusion (Flexas et al., 2021). Therefore, variations in the cell wall may also be the cause of the differences in photosynthetic performance between *P. antarctica* pop. Stream and pop. Beach.

Interestingly, both populations differed also in the content and responsivity (changes in the content) of key protective molecules such as carotenoids of the xanthophyll cycle and α-tocopherol. A rise in the AZ/VAZ ratio in response to desiccation has typically been reported in photosynthetic organisms tolerant to desiccation, including chlorophytes, during cell water loss (Fernández-Marín et al., 2011; Fernández-Marín, Roach, et al., 2021). In response to controlled desiccation in darkness, both populations increased their AZ/VAZ ratio. This rise was, however, much more pronounced and only significant in *P. antarctica* pop. Stream. Both populations had also significantly different α-Toc/Chl content. *P. antarctica* pop. Beach showed values comparable to *P. crispa* samples from Maritime Antarctica i.e. 60–90 mmol $mol^{-1}$ Chl (Fernández-Marín, López-Pozo, et al. 2019). By contrast, *P. antarctica* pop. Stream showed very low average values below 20 mmol $mol^{-1}$ Chl. It seems likely that repetitive cycles of immersion/emersion, with the consequent sudden changes in light, may have favoured a dynamic thylakoid protection mechanism based on responsive xanthophyll cycle in pop. Stream. By contrast, higher irradiances, longer dry periods and contrasting temperatures are probably more frequent in the terrestrial (and always emerged) pop. Beach, and consequently relies on higher α-Toc/Chl content.

In summary, *P. antarctica* has an extraordinary capacity to succeed in harsh Antarctic ecosystems including very contrasting micro environments such as terrestrial supralittoral belt and fresh-water ephemeral streams. Importantly, our data suggest that, at least partially, its success relies on a constitutive and efficient protection of thylakoids with an extraordinary composition of lipids and a high content of photoprotective xanthophylls that, overall, may protect photosynthetic apparatus under severe desiccation and freezing conditions. The biochemical composition of *P. antarctica* thylakoids favours, with a high proportion of cylindrical DGDG, the presence of substantial amounts of

© 2024 The Authors.


1365313x, 0, Downloaded from https://onlinelibrary.wiley.com/doi/10.1111/tpj.16742 by Institution Nac De Investig Tec Agra, Wiley Online Library on [24/05/2024]. See the Terms and Conditions (https://onlinelibrary.wiley.com/terms-and-conditions) on Wiley Online Library for rules of use; OA articles are governed by the applicable Creative Commons License

TGDG and an almost complete desaturation of acyl chains. As a result, the potential for stress-induced (desiccation) lipid remodelling is severely limited. The plasticity of *P. antarctica* seemed to depend greatly on anatomical changes, thus engrossed cell walls are favoured in freshwater environments and on some biochemical changes, e.g., accumulation of α-Toc is favoured in terrestrial environments. Based on the plasticity that presents *P. antarctica* as well as the known wider distribution of other polar *Prasiola* spp. (Garrido-Benavent et al., 2017), future studies that analyse the anatomical and physiological plasticity traits in regard to their distribution would be of high interest.

## EXPERIMENTAL PROCEDURES

### Study site

The study was conducted in the surroundings of the Spanish Antarctic Research Station 'Base Antártica Española Juan Carlos I' (BAE JCI) in Livingston Island, South Shetland (62°40′ S, 60°23′ W) (Figure 1). Field sampling and measurements were done at the end of the summer between the 26th of February and the 17th of March 2022. Two different populations of *Prasiola* sp. living in very contrasting environments were evaluated: one with terrestrial habit living on a beach, above the shore and on an herbaceous Antarctic tundra composed mainly of *Deschampsia antarctica* close to a penguinery, located at the W of the BAE JCI (Site 1, Figure 1); the other with freshwater habit, lived in a small ephemeral stream located at the E of the BAE JCI (Site 2, Figure 1). The stream is born a few hundred metres above the sampling site in a glacial melting pool and the flow is intermittent during summertime. Both populations were in North-facing exposures (south hemisphere). However, the overall incident solar radiation was lower at the stream location where individuals were vertically attached to rocks and very frequently submerged under a few millimetre of water depth. In contrast, at the beach population the thalli were horizontally attached over the substrate and not submerged. To better characterise the microenvironment of each population the general conditions of these different areas were collected from the available data published on Antarctic streams and coastal areas close to small penguin colonies in nearby areas (Table S4).

### Meteorological conditions

Air temperature, vapour pressure deficit (VPD), precipitation intensity (10 min) and PFD recorded by the nearby meteorological station (AEMET) are shown in Figure 2 for the studied period. During this period, the air temperature ranged between −2.7 and +4.2°C and the average daily rainfall was 1.24 mm day$^{-1}$. Atmospheric RH was on average 81% and, as a result, VPD was never higher than 0.3 kPa. The sky was mostly cloudy with a cumulative daily irradiance, on average, of 13.01 mol photons m$^{-2}$ day$^{-1}$ and with radiation peaks of 1400 μmol m$^{-2}$ s$^{-1}$.

### Molecular identification of *Prasiola* samples

Four samples (two collected at each site) were used for molecular identification. DNA extraction was carried out using the E.Z.N.A.® DNA soil Kit (Omega Bio-tek, Norcross, GA, USA) following the manufacturer's instructions. A fragment of the ribulose-1,5-bisphosphate carboxylase/oxygenase large subunit gene (*rbc*L), optimal to infer phylogenetic relationships in the genus (Moniz et al., 2012) was used, as well as the plastid-encoded *tufA* gene as a second molecular marker. Amplification was carried out using the primer pairs *rbc*L-pras-F and *rbc*L-pras-R and *tuf*AF-pras and *tuf*AR-pras respectively (Garrido-Benavent et al., 2018) using GE Healthcare illustra™ PuReTaq Ready-To-GoTM PCR Beads (GE Healthcare, Chicago, IL, USA). The reaction conditions were as follows: denaturation at 95°C for 5 min, followed by 35 cycles of denaturation at 94°C for 1 min, annealing at 55°C for 1 min and extension at 72°C for 2 min (final extension at 72°C for 10 min).

### Experimental design

Five different blocks of measurements were conducted. First, we took samples randomly from both populations for a general characterisation: anatomically and in terms of the photosynthetic pigment composition. Second, we compared photochemical (chloroplast electron transport) and photosynthetic (carbon fixation) efficiencies under different controlled conditions. Third, we evaluated the capability of both populations to tolerate different sub-zero temperatures and assessed their ice nucleation temperatures (*Experiment 1*). Fourth, we checked the capability of both populations to withstand different dehydration extents in the lab (*Experiment 2*). Finally, we conducted a controlled desiccation experiment to evaluate the differences among both populations on desiccation rate and on the subsequent biochemical adjustments at chloroplast level by analysing photosynthetic pigments, tocochromanols and plastid lipids (*Experiment 3*). All the experiments were conducted in Antarctica (*ex situ* in the lab of the BAE JCI, very close to the collection sites and with fresh collected material). For biochemical analyses, samples were kept frozen at −80°C and then analysed in our lab at the UPV/EHU. Frozen samples were freeze dried with a Heto PowerDry LL3000 freeze dryer (Thermo Fisher Scientific USA) for 72 h. Then, aliquots of lyophilised material (10–15 mg for lipids and 5 mg for pigments) were grinded using a Mixer Mill MM 400 (Retsch™, Germany) with two stainless steel G200 precision balls of 5 mm diameter and a bundle of 1 mm glass beads per Eppendorf tubes of 2 ml capacity.

In *Experiment 1*, we evaluated the extent of tolerance to subzero temperatures by subjecting wet samples of both populations to controlled cooling and rewarming profiles. Specifically, small thalli ($n$ = 6 per population) were put over wet paper into individual wells within a custom-made thermoelectric device (International Patent WO2024028532). Briefly, in this device, several Peltier elements are joined on a thermal block (made of aluminium and thermally isolated from outside). The thermal block is controlled by software to regulate the desired temperature treatments. Starting temperature was set to +15°C, initially dropped to 0°C in 30 min and then decreased at a cooling rate of 8 K h$^{-1}$ to a target temperature of either −6, −12 or − 18°C (see the Data S1 for further details). Maximal photochemical efficiency of PSII ($F_v/F_m$) before freezing and after ≥4 h of rewarming at 15°C were measured to estimate the freezing tolerance as % of values obtained at time zero. To determine ice nucleation temperature, we used the same device and compare temperature registered by a reference thermocouple (TL0260; PerfectPrime) and another attached to each sample, along a cooling treatment (cooling rate 8 K h$^{-1}$). Temperatures were registered in a CR 1000X; Campbell Scientific data logger every second. By subtracting sample temperature from the reference, ice nucleation temperature was determined at the onset of the exothermic peak.

In *Experiment 2* we assessed the tolerance of both populations to dehydration treatments of three different severities following the 'Falcon test' method described in López-Pozo et al. (2019). Briefly, fully hydrated samples were subjected to three different

© 2024 The Authors.


1365313x, 0, Downloaded from https://onlinelibrary.wiley.com/doi/10.1111/tpj.16742 by Institution Nac De Investig Tec Agra, Wiley Online Library on [24/05/2024]. See the Terms and Conditions (https://onlinelibrary.wiley.com/terms-and-conditions) on Wiley Online Library for rules of use; OA articles are governed by the applicable Creative Commons License

RHs: 75, 50 and ≤10% and then rehydrated. The RWC (estimated as % of actual water content to maximum water content ratio) and $F_v/F_m$ were monitored at time 0, after 48 h of dehydration and after 24 h of rehydration. We used three replicates per treatment (nine for species, in total). Whole experiment was conducted in darkness and at approximately +20°C.

In *Experiment 3*, we conducted a detailed monitoring of dehydration ratio, evolution of $F_v/F_m$ and dynamics in photosynthetic pigments, tocochromanols and chloroplast lipids, during a controlled dehydration of 40 h at 50% RH and at +4°C, in darkness and in a hermetic box. Water content and $F_v/F_m$ were recorded at times: 0, 1, 2, 5, 14, 24 and 40 h. Samples for biochemical analyses were collected at 36 h in two sets of samples: controls (were kept hydrated and at +4°C) and treatments (were incubated at 50% RH). Four to six replicates were measured per each time point and population.

### Light microscopy

Small fragments of *P. antarctica* samples were fixed under vacuum pressure with glutaraldehyde 4% and paraformaldehyde 2% in a 0.1 M phosphate buffer (pH 7.4) in the BAE JCI lab and transported in this medium to Spain. We then followed the fixation and inclusion procedure described in Tomás et al. (2013). Finally, semi-thin cross-sections (1 μm) were stained with 1% toluidine blue and viewed under an Olympus BX41 light microscope. Images taken with a Nikon DS-Fi1 camera were analysed with ImageJ 1.53c software (Wayne Rasband, National Institutes of Health, Bethesda, MD, USA). We used four different biological samples per population. Around 150 μm length of cross-section (~30–40 cells) were analysed per sample, where the average cell width, cell height and blade height were measured, as well as the total area occupied by cells and total blade area.

### Chlorophyll *a* fluorescence

Maximal photochemical efficiency of PSII in dark acclimated samples was measured with a portable modulated Plant Stress Kit fluorometer (Opti-Sciences, Hudson NH, USA) as described in García-Plazaola, Arzac, et al. (2022). Chloroplast ETR was estimated from YII measurements with a PAM 2500 (Heinz Walz GmbH, Effeltrich, Germany). This parameter was calculated as $ETR = \Phi_{PSII} \times PAR \times \alpha \times \beta$, where $\Phi_{PSII}$ is the effective quantum yield of PSII, PAR is the photosynthetic active radiation, $\alpha$ is the absorptance of the leaf, measured using a plant stress kit fluorometer and $\beta$ is the proportion of total incoming radiation absorbed by PSII, assumed the standard 0.5. The $\alpha$ value for *P. antarctica* pop. Beach was 0.838 and for pop. Stream was 0.844. RLCs were made at 4, 10, 15, 20 and 25°C in the BAE JCI lab. Each *P. antarctica* thallus was placed on a small petri dish. The petri dish was incubated in a thermostated water bath to keep the desired temperature during the measurement using the custom-made devices described in *Experiment 1*. The PAR used ranged from 0 to 2000 μmol photons $m^{-2}$ $s^{-1}$. RLCs were analysed according to Ralph and Gademann (2005), using the exponential model of (Platt et al., 1980) and the parameters maximum electron transport rate ($ETR_{max}$), apparent quantum efficiency for electron transport and minimum saturating irradiance ($E_k$) were determined. In the cases where down-regulation of PSII efficiency was detected, this value was also calculated.

### Gas exchange measurements

Measurements of $CO_2$ exchange in fresh samples of both populations of *P. antarctica* were done by using a LI-6800 system (LI-COR, Inc., Lincoln, NE, USA). $CO_2$ assimilation rate ($A_N$) was recorded at steady state conditions at 500 μmol photons $m^{-2}$ $s^{-1}$ and were normalised for the area of the cuvette covered by the sample. A custom-made cuvette was created where the samples were placed between two plastic net layers, as in García-Plazaola, Arzac, et al. (2022). The chamber was closed around this structure obtaining a proper closure with a leakage close to zero. $A_N$ was recorded at different temperatures, adjusting the block temperature at: 4, 10, 15, 20 and 25°C. To deepen the biochemical properties of *P. antarctica* $A_{N500}C_c$ curves were measured at 20°C. First, non-stomatal diffusion conductance ($g_{nsd}$) was calculated according to Harley et al. (1992), as analogous to mesophyll conductance ($g_m$) in higher plants (Carriquí et al., 2019). Considering that algae do not present stomata, we substituted $C_i$ with $C_a$ in the formula (Perera-Castro et al., 2020). We estimated $\Gamma^*$ from Bernacchi et al. (2001), considering that we measured photosynthesis at 20°C. $R_d$ was obtained assuming 50% of dark respiration from light curves (Sharkey, 2016). The averaged values of the raw data employed to calculate $g_{nsd}$ is shown in Table S5. In addition, to increase the accuracy in the estimation of $g_{nsd}$ per replicate we calculated this parameter in each point of the $A_{N500}C_c$ curves, excluding the unreliable values (negative values or values of several orders of magnitude difference). From the $A_{N500}C_c$ curves we obtained the parameters maximum carboxylation rate ($V_{cmax}$) and ETR at saturating light ($J_{high}$) using the excel spreadsheet provided in Sharkey (2016), using the $g_{nsd}$ as $g_m$ and $R_d$ values obtained by other methods as inputs. Additionally, we have estimated the limitations to photosynthesis according to Grassi and Magnani (2005). We used as a proxy of $\delta A/\delta C_c$ the quotient $A_N/C_c$ at 400 μmol $CO_2$ $mol^{-1}$ (Perera-Castro et al., 2020).

### High-performance liquid chromatography analyses

For photosynthetic pigments and tocopherol analyses, exact weight of approximately 5 mg per replicate was doubly extracted in pure acetone buffered with $CaCO_3$ (2 ml final volume). After centrifugation at 16 000 *g* the supernatant was filtered through a 0.2 μm polytetrafluoroethylene filter and then injected in a HPLC system. We used a reverse phase C18 column (Waters, Milford, MA, USA), a Waters 996 PDA detector and a Waters 474 fluorescence detector, following the method described in García-Plazaola and Becerril (1999).

### Quantification of polar lipids by Q-TOF

Chloroplast lipids were analysed from freeze dried and powdered material. We followed Gasulla et al. (2013) for the extraction procedure of polar lipids. Briefly, a first extraction with 1 ml of $CHCl_3$:MeOH (1:2, v/v) was done and the organic phase was collected. The extraction was repeated around three times with 1 ml of $CHCl_3$:MeOH (2:1, v/v) until the pellet turned white. To the combined organic phases, pure chloroform and aqueous ammonium acetate 0.3 M were added to obtain an organic phase of $CHCl_3$:MeOH:$C_2H_7NO_2$ (2:1:0.75, v/v) and left overnight at −20°C. Afterwards, the organic phase was harvested and evaporated completely under a stream of $N_2$. Finally, the lipids were dissolved in 1 ml of $CHCl_3$, transferred to a 2.0 ml clear glass vial and vacuum dried at room temperature (SPD 121P; Speed-Vac, Thermo Scientific Savant, NY, USA).

Quantification of phospholipids and glycolipids was performed by the Kansas Lipidomics Research Center at Kansas State University. Briefly, samples were dissolved in 1 ml of chloroform. Aliquots were mixed with internal standards and solvents as described in Shiva et al. (2013). Internal standards are indicated in Data S2. Lipid measurements were performed using a Sciex 4000 Q TRAP using the acquisition and data processing parameters

© 2024 The Authors.


1365313x, 0, Downloaded from https://onlinelibrary.wiley.com/doi/10.1111/tpj.16742 by Institution Nac De Investig Tec Agra, Wiley Online Library on [24/05/2024]. See the Terms and Conditions (https://onlinelibrary.wiley.com/terms-and-conditions) on Wiley Online Library for rules of use; OA articles are governed by the applicable Creative Commons License

indicated in Data S2. Internal standards were from the same class, or for classes without available internal standards: PC was used for DGTS, LysoPC for MGTS and DGDG 18:0/18:0 for TGDG and TeGDG. Factors to correct for the difference in the response of the instrument to MGDG and DGDG analytes versus their standards were applied.

### Statistical analyses

To analyse the population characterisation a one-way ANOVA was performed with the population as a factor. To analyse each experiment, two-way ANOVAs were carried out to detect the main effects of population and treatment and their interaction. The homogeneity of variances was checked by Levene's test and whether the residuals followed a normal distribution were checked by Kolmogorov–Smirnov test. If necessary, a transformation was performed. Duncan post-hoc was used to detect differences among treatments. Unless stated otherwise, $P < 0.05$ was considered significant. Statistical analyses were performed with SPSS v28.0.

## AUTHOR CONTRIBUTIONS

BF-M and JIG-P planned and designed the experiments. MIA, JM-A, AdlR, FC-M, JIG-P and BF-M performed the experiments. MIA, JM-A, JIG-P and BF-M wrote the manuscript. All authors contributed to the final version of the manuscript.

## ACKNOWLEDGEMENTS

These results have been partially obtained at the 'Spanish Antarctic Station Juan Carlos I' after having accessed during the 2021–2022 Spanish Antarctic Campaign. Jose Vicente Albero and the Antarctic AEMET Team are acknowledged for providing meteorological data. The extraordinary support received at the BAE JCI Station and during the campaign from the 'Unidad de Tecnología Marina-UTM' and the 'Comité Polar Español CPE' is also deeply acknowledged, with special mention to Joan Riba because of his positive attitude and troubleshooting capability along the whole campaign. The authors thank for technical and human support provided by the analytical and high-resolution microscopy in biomedicine service SGIker (UPV/EHU/ ERDF, EU). This research was funded through the following projects: PGC2018-093824-B-C41, PGC2018-093824-B-C44 and PID2022-139455NB-C32 funded by MCIN/AEI/10.13039/501100011033 and by 'ERDF A way of making Europe'; PID2019-105469RB-C22 funded by MCIN/AEI/10.13039/501100011033/FEDER, UE; and by IT1648-22 funded by the Basque Government. MIA enjoyed a pre-doctoral grant from the Basque Government. BF-M enjoyed the RYC2021-031321-I grant funded by MCIN/AEI/10.13039/501100011033 and by the European Union NextGenerationEU/PRTR. FC-M enjoyed a pre-doctoral fellowship from the MCIN (PRE-2019-090011). The lipid profile data were acquired at Kansas Lipidomics Research Center (KLRC). Instrument acquisition and method development at KLRC was supported by Kansas INBRE (NIH Grant P20 RR16475 from the INBRE programme of the National Center for Research Resources), NSF EPSCoR grant EPS-0236913, Kansas Technology Enterprise Corporation and Kansas State University. We want to thank Usue Pérez-López for the assistance with the methodology of the $A_N/C_c$ curves and related parameters.

## CONFLICT OF INTEREST

All authors declare that there are no conflicts of interest.

## DATA AVAILABILITY STATEMENT

The data that supports the findings of this study are available in the supplementary material of this article and from the corresponding author upon request.

## SUPPORTING INFORMATION

Additional Supporting Information may be found in the online version of this article.

**Data S1.** Additional information regarding the freezing test methodology using the custom-made thermoelectric device.

**Data S2.** Molecular species composition data of analysed polar lipids obtained by the KLRC and measurement related parameters.

**Figure S1.** Light curves of $CO_2$ assimilation of *P. antarctica* at +4°C.

**Figure S2.** Correlation between electron transport rate and temperature in different populations of *P. antarctica*.

**Figure S3.** Correlation between chlorophyll *a* fluorescence and relative water content (RWC) in *P. antarctica* during controlled desiccation.

**Figure S4.** Molecular species composition of phospholipids in *P. antarctica* populations under controlled desiccation.

**Figure S5.** Fatty acid unsaturation of polar lipids analysed in *P. antarctica* populations under controlled desiccation.

**Table S1.** Photosynthetic parameters estimated from assimilation-$CO_2$ response curves (+20°C).

**Table S2.** Photosynthetic parameters estimated from the electron transport rate curves.

**Table S3.** Results of the two-way ANOVA performed for the photoprotection mechanisms.

**Table S4.** Proxy of the microenvironments of our studied *P. antarctica* populations, based on data obtained in the literature.

**Table S5.** Averaged values of raw data employed to calculate $g_{nsd}$ values according to the method in Harley *et al.* (1992).

## REFERENCES

**Abakumov, E.V.**, **Parnikoza, I.Y.**, **Zhianski, M.**, **Yaneva, R.**, **Lupachev, A.V.**, **Andreev, M.P. *et al.*** (2021) Ornithogenic factor of soil formation in Antarctica: a review. *Eurasian Soil Science*, **54**, 528–540.

**Aigner, S.**, **Glaser, K.**, **Arc, E.**, **Holzinger, A.**, **Schletter, M.**, **Karsten, U. *et al.*** (2020) Adaptation to aquatic and terrestrial environments in *Chlorella vulgaris* (Chlorophyta). *Frontiers in Microbiology*, **11**, 585836.

**Arisz, S.A.**, **Heo, J.-Y.**, **Koevoets, I.T.**, **Zhao, T.**, **van Egmond, P.**, **Meyer, A.J. *et al.*** (2018) DIACYLGLYCEROL ACYLTRANSFERASE1 contributes to freezing tolerance. *Plant Physiology*, **177**, 1410–1424.

**Bacior, M.**, **Harańczyk, H.**, **Nowak, P.**, **Kijak, P.**, **Marzec, M.**, **Fitas, J. *et al.*** (2022) Low-temperature investigation of residual water bound in free-living Antarctic *Prasiola crispa*. *Antarctic Science*, **34**, 389–400.

**Bacior, M.**, **Nowak, P.**, **Harańczyk, H.**, **Patryas, S.**, **Kijak, P.**, **Ligęzowska, A. *et al.*** (2017) Extreme dehydration observed in Antarctic *Turgidosculum complicatulum* and in *Prasiola crispa*. *Extremophiles*, **21**, 331–343.

**Becker, E.W.** (1982) Physiological studies on antarctic *Prasiola crispa* and *Nostoc commune* at low temperatures. *Polar Biology*, **1**, 99–104.

**Benson, A.A.**, **Wiser, R.**, **Ferrari, R.A.** & **Miller, J.A.** (1958) Photosynthesis of galactolipids. *Journal of the American Chemical Society*, **80**, 4740.

**Bernacchi, C.J.**, **Singsaas, E.L.**, **Pimentel, C.**, **Portis, A.R., Jr.** & **Long, S.P.** (2001) Improved temperature response functions for models of rubisco-limited photosynthesis. *Plant, Cell and Environment*, **24**, 253–259.

**Boisvenue, C.** & **Running, S.W.** (2006) Impacts of climate change on natural forest productivity – evidence since the middle of the 20th century. *Global Change Biology*, **12**, 862–882.

**Broady, P.A.** (1989) Survey of algae and other terrestrial biota at Edward VII peninsula, Marie Byrd Land. *Antarctic Science*, **1**, 215–224.

© 2024 The Authors.


1365313x, 0, Downloaded from https://onlinelibrary.wiley.com/doi/10.1111/tpj.16742 by Institution Nac De Investig Tec Agra, Wiley Online Library on [24/05/2024]. See the Terms and Conditions (https://onlinelibrary.wiley.com/terms-and-conditions) on Wiley Online Library for rules of use; OA articles are governed by the applicable Creative Commons License

**Brooks, S.T.**, **Jabour, J.**, **van den Hoff, J.** & **Bergstrom, D.M.** (2019) Our footprint on Antarctica competes with nature for rare ice-free land. *Nature Sustainability*, **2**, 185–190.

**Carriquí, M.**, **Roig-Oliver, M.**, **Brodribb, T.J.**, **Coopman, R.**, **Gill, W.**, **Mark, K.** ***et al.*** (2019) Anatomical constraints to nonstomatal diffusion conductance and photosynthesis in lycophytes and bryophytes. *The New Phytologist*, **222**, 1256–1270.

**Chng, C.-P.**, **Wang, K.**, **Ma, W.**, **Hsia, K.J.** & **Huang, C.** (2021) Chloroplast membrane lipid remodeling protects against dehydration by limiting membrane fusion and distortion. *Plant Physiology*, **188**, 526–539.

**Colesie, C.**, **Walshaw, C.V.**, **Sancho, L.G.**, **Davey, M.P.** & **Gray, A.** (2023) Antarctica's vegetation in a changing climate. *WIREs Climate Change*, **14**, e810.

**Davis, R.C.** (1981) Structure and function of two Antarctic terrestrial moss communities. *Ecological Monographs*, **51**, 125–143.

**Dubrasquet, H.**, **Garrido, I.**, **Bruning, P.**, **Reyes, J.** & **Guillemin, M.-L.** (2021) Building-up knowledge on green marine macroalgae diversity in the Western Antarctic peninsula: data from two molecular markers reveals numerous species with amphipolar distribution. *Cryptogamie, Algologie*, **42**(21–37).

**Durán, J.**, **Rodríguez, A.**, **Heiðmarsson, S.**, **Lehmann, J.R.K.**, **del Moral, Á.**, **Garrido-Benavent, I.** ***et al.*** (2021) Cryptogamic cover determines soil attributes and functioning in polar terrestrial ecosystems. *Science of the Total Environment*, **762**, 143169.

**Ernst, R.**, **Ejsing, C.S.** & **Antonny, B.** (2016) Homeoviscous adaptation and the regulation of membrane lipids. *Journal of Molecular Biology*, **428**, 4776–4791.

**Esteban, R.**, **Barrutia, O.**, **Artetxe, U.**, **Fernández-Marín, B.**, **Hernández, A.** & **García-Plazaola, J.I.** (2015) Internal and external factors affecting photosynthetic pigment composition in plants: a meta-analytical approach. *The New Phytologist*, **206**, 268–280.

**Fernández-Marín, B.**, **Arzac, M.I.**, **López-Pozo, M.**, **Laza, J.M.**, **Roach, T.**, **Stegner, M.** ***et al.*** (2021) Frozen in the dark: interplay of night-time activity of xanthophyll cycle, xylem attributes, and desiccation tolerance in fern resistance to winter. *Journal of Experimental Botany*, **72**, 3168–3184.

**Fernández-Marín, B.**, **Atherton, J.**, **Olascoaga, B.**, **Kolari, P.**, **Porcar-Castell, A.** & **García-Plazaola, J.I.** (2018) When the sun never sets: daily changes in pigment composition in three subarctic woody plants during the summer solstice. *Trees*, **32**, 615–630.

**Fernández-Marín, B.**, **Gago, J.**, **Clemente-Moreno, M.J.**, **Flexas, J.**, **Gulías, J.** & **García-Plazaola, J.I.** (2019) Plant pigment cycles in the high-Arctic Spitsbergen. *Polar Biology*, **42**, 675–684.

**Fernández-Marín, B.**, **Gulías, J.**, **Figueroa, C.M.**, **Iñiguez, C.**, **Clemente-Moreno, M.J.**, **Nunes-Nesi, A.** ***et al.*** (2020) How do vascular plants perform photosynthesis in extreme environments? An integrative ecophysiological and biochemical story. *The Plant Journal*, **101**, 979–1000.

**Fernández-Marín, B.**, **López-Pozo, M.**, **Perera-Castro, A.V.**, **Arzac, M.I.**, **Sáenz-Ceniceros, A.**, **Colesie, C.** ***et al.*** (2019) Symbiosis at its limits: ecophysiological consequences of lichenization in the genus *Prasiola* in Antarctica. *Annals of Botany*, **124**, 1211–1226.

**Fernández-Marín, B.**, **Míguez, F.**, **Becerril, J.M.** & **García-Plazaola, J.I.** (2011) Dehydration-mediated activation of the xanthophyll cycle in darkness: is it related to desiccation tolerance? *Planta*, **234**, 579–588.

**Fernández-Marín, B.**, **Nadal, M.**, **Gago, J.**, **Fernie, A.R.**, **López-Pozo, M.**, **Artetxe, U.** ***et al.*** (2020) Born to revive: molecular and physiological mechanisms of double tolerance in a paleotropical and resurrection plant. *The New Phytologist*, **226**, 741–759.

**Fernández-Marín, B.**, **Neuner, G.**, **Kuprian, E.**, **Laza, J.M.**, **García-Plazaola, J.I.** & **Verhoeven, A.** (2018) First evidence of freezing tolerance in a resurrection plant: insights into molecular mobility and zeaxanthin synthesis in the dark. *Physiologia Plantarum*, **163**, 472–489.

**Fernández-Marín, B.**, **Roach, T.**, **Verhoeven, A.** & **García-Plazaola, J.I.** (2021) Shedding light on the dark side of xanthophyll cycles. *The New Phytologist*, **230**, 1336–1344.

**Flaim, G.**, **Obertegger, U.** & **Guella, G.** (2012) Changes in galactolipid composition of the cold freshwater dinoflagellate *Borghiella dodgei* in response to temperature. *Hydrobiologia*, **698**, 285–293.

**Flexas, J.**, **Clemente-Moreno, M.J.**, **Bota, J.**, **Brodribb, T.J.**, **Gago, J.**, **Mizokami, Y.** ***et al.*** (2021) Cell wall thickness and composition are involved in photosynthetic limitation. *Journal of Experimental Botany*, **72**, 3971–3986.

**Foyer, C.H.**, **Descourvières, P.** & **Kunert, K.J.** (1994) Protection against oxygen radicals: an important defence mechanism studied in transgenic plants. *Plant, Cell and Environment*, **17**, 507–523.

**García-Plazaola, J.I.**, **Arzac, M.I.**, **Brazales, L.**, **Fernández, J.**, **Laza, J.M.**, **Vilas, J.L.** ***et al.*** (2022) Freezing and desiccation tolerance in the Antarctic bangiophyte *Pyropia endiviifolia* (Rhodophyta): a chicken and egg problem? *European Journal of Phycology*, **58**, 377–389.

**García-Plazaola, J.I.** & **Becerril, J.M.** (1999) A rapid high-performance liquid chromatography method to measure lipophilic antioxidants in stressed plants: simultaneous determination of carotenoids and tocopherols. *Phytochemical Analysis*, **10**, 307–313.

**García-Plazaola, J.I.**, **López-Pozo, M.** & **Fernández-Marín, B.** (2022) Xanthophyll cycles in the juniper haircap moss (*Polytrichum juniperinum*) and Antarctic hair grass (*Deschampsia antarctica*) on Livingston Island (South Shetland Islands, maritime Antarctica). *Polar Biology*, **45**, 1247–1256.

**Garrido-Benavent, I.**, **de los Ríos, A.**, **Fernández-Mendoza, F.** & **Pérez-Ortega, S.** (2018) No need for stepping stones: direct, joint dispersal of the lichen-forming fungus *Mastodia tessellata* (Ascomycota) and its photobiont explains their bipolar distribution. *Journal of Biogeography*, **45**, 213–224.

**Garrido-Benavent, I.**, **Pérez-Ortega, S.** & **de los Ríos, A.** (2017) From Alaska to Antarctica: species boundaries and genetic diversity of *Prasiola* (Trebouxiophyceae), a foliose chlorophyte associated with the bipolar lichen-forming fungus *Mastodia tessellata*. *Molecular Phylogenetics and Evolution*, **107**, 117–131.

**Gasulla, F.**, **Barreno, E.**, **Parages, M.L.**, **Cámara, J.**, **Jiménez, C.**, **Dörmann, P.** ***et al.*** (2016) The role of phospholipase D and MAPK signaling cascades in the adaption of lichen microalgae to desiccation: changes in membrane lipids and phosphoproteome. *Plant & Cell Physiology*, **57**, 1908–1920.

**Gasulla, F.**, **García-Plazaola, J.I.**, **López-Pozo, M.** & **Fernández-Marín, B.** (2019) Evolution, biosynthesis and protective roles of oligogalactolipids: key molecules for terrestrial photosynthesis? *Environmental and Experimental Botany*, **164**, 135–148.

**Gasulla, F.**, **vom Dorp, K.**, **Dombrink, I.**, **Zähringer, U.**, **Gisch, N.**, **Dörmann, P.** ***et al.*** (2013) The role of lipid metabolism in the acquisition of desiccation tolerance in *Craterostigma plantagineum*: a comparative approach. *The Plant Journal*, **75**, 726–741.

**González-Herrero, S.**, **Barriopedro, D.**, **Trigo, R.M.**, **López-Bustins, J.A.** & **Oliva, M.** (2022) Climate warming amplified the 2020 record-breaking heatwave in the Antarctic peninsula. *Communications Earth & Environment*, **3**, 122.

**Graeve, M.**, **Kattner, G.**, **Wiencke, C.** & **Karsten, U.** (2002) Fatty acid composition of Arctic and Antarctic macroalgae: indicator of phylogenetic and trophic relationships. *Marine Ecology Progress Series*, **231**, 67–74.

**Grassi, G.** & **Magnani, F.** (2005) Stomatal, mesophyll conductance and biochemical limitations to photosynthesis as affected by drought and leaf ontogeny in ash and oak trees. *Plant, Cell and Environment*, **28**, 834–849.

**Grudzinski, W.**, **Nierzwicki, L.**, **Welc, R.**, **Reszczynska, E.**, **Luchowski, R.**, **Czub, J.** ***et al.*** (2017) Localization and orientation of xanthophylls in a lipid bilayer. *Scientific Reports*, **7**, 9619.

**Harley, P.C.**, **Loreto, F.**, **Di Marco, G.** & **Sharkey, T.D.** (1992) Theoretical considerations when estimating the mesophyll conductance to $CO_2$ flux by analysis of the response of photosynthesis to $CO_2$. *Plant Physiology*, **98**, 1429–1436.

**Hartmann, A.**, **Holzinger, A.**, **Ganzera, M.** & **Karsten, U.** (2016) Prasiolin, a new UV-sunscreen compound in the terrestrial green macroalga *Prasiola calophylla* (Carmichael ex Greville) Kützing (Trebouxiophyceae, Chlorophyta). *Planta*, **243**, 161–169.

**Havaux, M.** (1998) Carotenoids as membrane stabilizers in chloroplasts. *Trends in Plant Science*, **3**, 147–151.

**Holzinger, A.**, **Herburger, K.**, **Blaas, K.**, **Lewis, L.A.** & **Karsten, U.** (2017) The terrestrial green macroalga *Prasiola calophylla* (Trebouxiophyceae, Chlorophyta): ecophysiological performance under water-limiting conditions. *Protoplasma*, **254**, 1755–1767.

**Holzinger, A.** & **Karsten, U.** (2013) Desiccation stress and tolerance in green algae: consequences for ultrastructure, physiological and molecular mechanisms. *Frontiers in Plant Science*, **4**, 327.

**Holzinger, A.**, **Karsten, U.**, **Lütz, C.** & **Wiencke, C.** (2006) Ultrastructure and photosynthesis in the supralittoral green macroalga *Prasiola crispa* from Spitsbergen (Norway) under UV exposure. *Phycologia*, **45**, 168–177.

© 2024 The Authors.
*The Plant Journal* published by Society for Experimental Biology and John Wiley & Sons Ltd.,


1365313x, 0, Downloaded from https://onlinelibrary.wiley.com/doi/10.1111/tpj.16742 by Institution Nac De Investig Tec Agra, Wiley Online Library on [24/05/2024]. See the Terms and Conditions (https://onlinelibrary.wiley.com/terms-and-conditions) on Wiley Online Library for rules of use; OA articles are governed by the applicable Creative Commons License

**Huiskes, A.H.L.**, **Gremmen, N.J.M.** & **Francke, J.W.** (1997) The delicate stability of lichen symbiosis: comparative studies on the photosynthesis of the lichen *Mastodia tesselata* and its free-living phycobiont, the alga *Prasiola crispa*. In: Battaglia, B., Valencia, J. & Walton, D.W.H. (Eds.) *Antarctic communities: species, structure and survival*. Cambridge: Cambridge University Press, pp. 234–240.

**Huner, N.P.A.**, **Öquist, G.** & **Sarhan, F.** (1998) Energy balance and acclimation to light and cold. *Trends in Plant Science*, **3**, 224–230.

**Hüner, N.P.A.**, **Smith, D.R.**, **Cvetkovska, M.**, **Zhang, X.**, **Ivanov, A.G.**, **Szyszka-Mroz, B.** ***et al.*** (2022) Photosynthetic adaptation to polar life: energy balance, photoprotection and genetic redundancy. *Journal of Plant Physiology*, **268**, 153557.

**Jackson, A.E.** & **Seppelt, R.D.** (1995) The accumulation of proline in *Prasiola crispa* during winter in Antarctica. *Physiologia Plantarum*, **94**, 25–30.

**Jacob, A.**, **Kirst, G.O.**, **Wiencke, C.** & **Lehmann, H.** (1991) Physiological responses of the antarctic green alga *Prasiola crispa* ssp. *Antarctica* to salinity stress. *Journal of Plant Physiology*, **139**, 57–62.

**Jacob, A.**, **Lehmann, H.**, **Kirst, G.O.** & **Wiencke, C.** (1992) Changes in the ultrastructure of *Prasiola crispa* ssp. *Antarctica* under salinity stress. *Botanica Acta: Journal of the German Botanical Society*, **105**, 41–46.

**Jacob, A.**, **Wiencke, C.**, **Lehmann, H.** & **Kirst, G.O.** (1992) Physiology and ultrastructure of desiccation in the green alga *Prasiola crispa* from Antarctica. *Botanica Marina*, **35**, 297–304.

**Kang, E.J.**, **Scrosati, R.A.** & **Garbary, D.J.** (2013) Physiological ecology of photosynthesis in *Prasiola stipitata* (Trebouxiophyceae) from the bay of Fundy, Canada. *Phycological Research*, **61**, 208–216.

**Kappen, L.**, **Schroeter, B.**, **Green, T.G.A.** & **Seppelt, R.D.** (1998) Chlorophyll *a* fluorescence and $CO_2$ exchange of *Umbilicaria aprina* under extreme light stress in the cold. *Oecologia*, **113**, 325–331.

**Kosugi, M.**, **Katashima, Y.**, **Aikawa, S.**, **Tanabe, Y.**, **Kudoh, S.**, **Kashino, Y.** ***et al.*** (2010) Comparative study on the photosynthetic properties of *Prasiola* (chlorophyceae) and *Nostoc* (cyanophyceae) from antarctic and non-antarctic sites. *Journal of Phycology*, **46**, 466–476.

**Kosugi, M.**, **Ozawa, S.-I.**, **Takahashi, Y.**, **Kamei, Y.**, **Itoh, S.**, **Kudoh, S.** ***et al.*** (2020) Red-shifted chlorophyll *a* bands allow uphill energy transfer to photosystem II reaction centers in an aerial green alga, *Prasiola crispa*, harvested in Antarctica. *Biochimica et Biophysica Acta*, **1861**, 148139.

**Kromdijk, J.**, **Głowacka, K.**, **Leonelli, L.**, **Gabilly, S.T.**, **Iwai, M.**, **Niyogi, K.K.** ***et al.*** (2016) Improving photosynthesis and crop productivity by accelerating recovery from photoprotection. *Science*, **354**, 857–861.

**Leblond, J.D.**, **Dahmen, J.L.** & **Evens, T.J.** (2010) Mono- and digalactosyldiacylglycerol composition of dinoflagellates. IV. Temperature-induced modulation of fatty acid regiochemistry as observed by electrospray ionization/mass spectrometry. *European Journal of Phycology*, **45**, 13–18.

**Leliaert, F.**, **Smith, D.R.**, **Moreau, H.**, **Herron, M.D.**, **Verbruggen, H.**, **Delwiche, C.F.** ***et al.*** (2012) Phylogeny and molecular evolution of the green algae. *Critical Reviews in Plant Sciences*, **31**, 1–46.

**Levin, G.**, **Kulikovsky, S.**, **Liveanu, V.**, **Eichenbaum, B.**, **Meir, A.**, **Isaacson, T.** ***et al.*** (2021) The desert green algae *Chlorella ohadii* thrives at excessively high light intensities by exceptionally enhancing the mechanisms that protect photosynthesis from photoinhibition. *The Plant Journal*, **106**, 1260–1277.

**López-Pozo, M.**, **Flexas, J.**, **Gulías, J.**, **Carriquí, M.**, **Nadal, M.**, **Perera-Castro, A.V.** ***et al.*** (2019) A field portable method for the semi-quantitative estimation of dehydration tolerance of photosynthetic tissues across distantly related land plants. *Physiologia Plantarum*, **167**, 540–555.

**Lud, D.**, **Buma, A.G.J.**, **Van De Poll, W.**, **Moerdijk, T.C.W.** & **Huiskes, A.H.L.** (2001) DNA damage and photosynthetic performance in the antarctic terrestrial alga *Prasiola crispa* ssp. *antarctica* (Chlorophyta) under manipulated UV-B radiation. *Journal of Phycology*, **37**, 459–467.

**Lukashanets, D.A.**, **Convey, P.**, **Borodin, O.I.**, **Miamin, V.Y.**, **Hihiniak, Y.H.**, **Gaydashov, A.A.** ***et al.*** (2021) Eukarya biodiversity in the Thala Hills, East Antarctica. *Antarctic Science*, **33**, 605–623.

**Lukashanets, D.A.**, **Hihiniak, Y.H.** & **Miamin, V.Y.** (2022) Extremely high abundances of *Prasiola crispa*-associated micrometazoans in East Antarctica. *Polar Research*, **41**, 17781.

**Magney, T.S.**, **Logan, B.A.**, **Reblin, J.S.**, **Boelman, N.T.**, **Eitel, J.U.H.**, **Greaves, H.E.** ***et al.*** (2017) Xanthophyll cycle activity in two prominent arctic shrub species. *Arctic, Antarctic, and Alpine Research*, **49**, 277–289.

**Mendiola-Morgenthaler, L.**, **Eichenberger, W.** & **Boschetti, A.** (1985) Isolation of chloroplast envelopes from *Chlamydomonas*. Lipid and polypeptide composition. *Plant Science*, **41**, 97–104.

**Moniz, M.B.J.**, **Rindi, F.**, **Novis, P.M.**, **Broady, P.A.** & **Guiry, M.D.** (2012) Molecular phylogeny of antarctic *Prasiola* (Prasiolales, Trebouxiophyceae) reveals extensive cryptic diversity. *Journal of Phycology*, **48**, 940–955.

**Montero, O.**, **Velasco, M.**, **Miñón, J.**, **Marks, E.A.N.**, **Sanz-Arranz, A.** & **Rad, C.** (2021) Differential membrane lipid profiles and vibrational spectra of three edaphic algae and one cyanobacterium. *International Journal of Molecular Sciences*, **22**, 11277.

**Morita, R.Y.** (1975) Psychrophilic bacteria. *Bacteriological Reviews*, **39**, 144–167.

**Muggia, L.**, **Leavitt, S.** & **Barreno, E.** (2018) The hidden diversity of lichenised Trebouxiophyceae (Chlorophyta). *Phycologia*, **57**, 503–524.

**Nadal, M.**, **Perera-Castro, A.V.**, **Gulías, J.**, **Farrant, J.M.** & **Flexas, J.** (2021) Resurrection plants optimize photosynthesis despite very thick cell walls by means of chloroplast distribution. *Journal of Experimental Botany*, **72**, 2600–2610.

**Ochyra, R.**, **Lewis Smith, R.I.** & **Bednarek-Ochyra, H.** (2008) *The illustrated moss flora of Antarctica*. Cambridge: Cambridge University Press.

**Ohtani, S.**, **Kanda, H.** & **Ino, Y.** (1990) Microclimate data measured at the Yukidori Valley, Langhovde, Antarctica in 1988–1989. *JARE Data Reports*, **152**, 1–216.

**Ort, D.R.** (2001) When there is too much light. *Plant Physiology*, **125**, 29–32.

**Øvstedal, D.O.** & **Lewis Smith, R.I.** (2001) *Lichens of Antarctica and South Georgia: a guide to their identification and ecology*. Cambridge: Cambridge University Press.

**Peat, H.J.**, **Clarke, A.** & **Convey, P.** (2007) Diversity and biogeography of the Antarctic flora. *Journal of Biogeography*, **34**, 132–146.

**Pellizzari, F.**, **Silva, M.C.**, **Silva, E.M.**, **Medeiros, A.**, **Oliveira, M.C.**, **Yokoya, N.S.** ***et al.*** (2017) Diversity and spatial distribution of seaweeds in the South Shetland Islands, Antarctica: an updated database for environmental monitoring under climate change scenarios. *Polar Biology*, **40**, 1671–1685.

**Perera-Castro, A.V.** & **Flexas, J.** (2023) The ratio of electron transport to assimilation ($ETR/A_N$): underutilized but essential for assessing both equipment's proper performance and plant status. *Planta*, **257**, 29.

**Perera-Castro, A.V.**, **Flexas, J.**, **González-Rodríguez, Á.M.** & **Fernández-Marín, B.** (2021) Photosynthesis on the edge: photoinhibition, desiccation and freezing tolerance of Antarctic bryophytes. *Photosynthesis Research*, **149**, 135–153.

**Perera-Castro, A.V.**, **Waterman, M.J.**, **Turnbull, J.D.**, **Ashcroft, M.B.**, **McKinley, E.**, **Watling, J.R.** ***et al.*** (2020) It is hot in the sun: Antarctic mosses have high temperature optima for photosynthesis despite cold climate. *Frontiers in Plant Science*, **11**, 1178.

**Pérez-Ortega, S.**, **de los Ríos, A.**, **Crespo, A.** & **Sancho, L.G.** (2010) Symbiotic lifestyle and phylogenetic relationships of the bionts of *Mastodia tesselata* (Ascomycota, *incertae sedis*). *American Journal of Botany*, **97**, 738–752.

**Platt, T.**, **Gallegos, C.L.** & **Harrison, W.G.** (1980) Photoinhibition of photosynthesis in natural assemblages of marine phytoplankton. *Journal of Marine Research*, **38**, 687–701.

**Ralph, P.J.** & **Gademann, R.** (2005) Rapid light curves: a powerful tool to assess photosynthetic activity. *Aquatic Botany*, **82**, 222–237.

**Ramírez, R.**, **Carmona, J.** & **Martorell, C.** (2007) Microhabitat and morphometric variation in two species of *Prasiola* (Prasiolales, Chlorophyta) from streams in central Mexico. *Aquatic Ecology*, **41**, 161–168.

**Richter, D.**, **Matuła, J.**, **Urbaniak, J.**, **Waleron, M.** & **Czerwik-Marcinkowska, J.** (2017) Molecular, morphological and ultrastructural characteristics of *Prasiola crispa* (Lightfoot) Kützing (Chlorophyta) from Spitsbergen (Arctic). *Polar Biology*, **40**, 379–397.

**Rindi, F.**, **McIvor, L.**, **Sherwood, A.R.**, **Friedl, T.**, **Guiry, M.D.** & **Sheath, R.G.** (2007) Molecular phylogeny of the green algal order Prasiolales (Trebouxiophyceae, Chlorophyta). *Journal of Phycology*, **43**, 811–822.

**Robinson, S.A.**, **Wasley, J.** & **Tobin, A.K.** (2003) Living on the edge – plants and global change in continental and maritime Antarctica. *Global Change Biology*, **9**, 1681–1717.

**Roig-Oliver, M.**, **Douthe, C.**, **Bota, J.** & **Flexas, J.** (2021) Cell wall thickness and composition are related to photosynthesis in Antarctic mosses. *Physiologia Plantarum*, **173**, 1914–1925.

© 2024 The Authors.


1365313x, 0, Downloaded from https://onlinelibrary.wiley.com/doi/10.1111/tpj.16742 by Institution Nac De Investig Tec Agra, Wiley Online Library on [24/05/2024]. See the Terms and Conditions (https://onlinelibrary.wiley.com/terms-and-conditions) on Wiley Online Library for rules of use; OA articles are governed by the applicable Creative Commons License

**Rolland, N.**, **Ferro, M.**, **Seigneurin-Berny, D.**, **Garin, J.**, **Block, M.** & **Joyard, J.** (2009) The chloroplast envelope proteome and lipidome. In: Sandelius, A.S. & Aronsson, H. (Eds.) *The chloroplast: interactions with the environment*. Berlin, Heidelberg: Springer Berlin Heidelberg, pp. 41–88.

**Sanders, W.B.** & **Masumoto, H.** (2021) Lichen algae: the photosynthetic partners in lichen symbioses. *The Lichenologist*, **53**, 347–393.

**Sato, N.**, **Tsuzuki, M.** & **Kawaguchi, A.** (2003) Glycerolipid synthesis in *Chlorella kessleri* 11h: I. Existence of a eukaryotic pathway. *Biochimica et Biophysica Acta*, **1633**, 27–34.

**Schroeter, B.**, **Green, T.G.A.**, **Kulle, D.**, **Pannewitz, S.**, **Schlensog, M.** & **Sancho, L.G.** (2012) The moss *Bryum argenteum* var. *muticum* Brid. Is well adapted to cope with high light in continental Antarctica. *Antarctic Science*, **24**, 281–291.

**Sharkey, T.D.** (2016) What gas exchange data can tell us about photosynthesis. *Plant, Cell and Environment*, **39**, 1161–1163.

**Shiva, S.**, **Vu, H.S.**, **Roth, M.R.**, **Zhou, Z.**, **Marepally, S.R.**, **Nune, D.S.** ***et al.*** (2013) Lipidomic analysis of plant membrane lipids by direct infusion tandem mass spectrometry. In: Munnik, T. & Heilmann, I. (Eds.) *Plant lipid signaling protocols*. Totowa, NJ: Humana Press, pp. 79–91.

**Smith, V.R.** & **Gremmen, N.J.M.** (2001) Photosynthesis in a sub-Antarctic shore-zone lichen. *The New Phytologist*, **149**, 291–299.

**Spain, O.** & **Funk, C.** (2022) Detailed characterization of the cell wall structure and composition of Nordic green microalgae. *Journal of Agricultural and Food Chemistry*, **70**, 9711–9721.

**Tomás, M.**, **Flexas, J.**, **Copolovici, L.**, **Galmés, J.**, **Hallik, L.**, **Medrano, H.** ***et al.*** (2013) Importance of leaf anatomy in determining mesophyll diffusion conductance to $CO_2$ across species: quantitative limitations and scaling up by models. *Journal of Experimental Botany*, **64**, 2269–2281.

**Verhoeven, A.**, **García-Plazaola, J.I.** & **Fernández-Marín, B.** (2018) Shared mechanisms of photoprotection in photosynthetic organisms tolerant to desiccation or to low temperature. *Environmental and Experimental Botany*, **154**, 66–79.

**Vieler, A.**, **Wilhelm, C.**, **Goss, R.**, **Süß, R.** & **Schiller, J.** (2007) The lipid composition of the unicellular green alga *Chlamydomonas reinhardtii* and the diatom *Cyclotella meneghiniana* investigated by MALDI-TOF MS and TLC. *Chemistry and Physics of Lipids*, **150**, 143–155.

**Walker, A.P.**, **Beckerman, A.P.**, **Gu, L.**, **Kattge, J.**, **Cernusak, L.A.**, **Domingues, T.F.** ***et al.*** (2014) The relationship of leaf photosynthetic traits – $V_{cmax}$ and $J_{max}$ – to leaf nitrogen, leaf phosphorus, and specific leaf area: a meta-analysis and modeling study. *Ecology and Evolution*, **4**, 3218–3235.

**Welti, R.**, **Li, W.**, **Li, M.**, **Sang, Y.**, **Biesiada, H.**, **Zhou, H.-E.** ***et al.*** (2002) Profiling membrane lipids in plant stress responses. Role of phospholipase D alpha in freezing-induced lipid changes in Arabidopsis. *The Journal of Biological Chemistry*, **277**, 31994–32002.

**Yoshihara, A.** & **Kobayashi, K.** (2022) Lipids in photosynthetic protein complexes in the thylakoid membrane of plants, algae, and cyanobacteria. *Journal of Experimental Botany*, **73**, 2735–2750.

**Yu, L.**, **Zhou, C.**, **Fan, J.**, **Shanklin, J.** & **Xu, C.** (2021) Mechanisms and functions of membrane lipid remodeling in plants. *The Plant Journal*, **107**, 37–53.

**Zębek, E.**, **Napiórkowska-Krzebietke, A.**, **Świątecki, A.** & **Górniak, D.** (2021) Biodiversity of periphytic cyanobacteria and algae assemblages in polar region: a case study of the vicinity of Arctowski polish Antarctic Station (King George Island, Antarctica). *Biodiversity and Conservation*, **30**, 2751–2771.

© 2024 The Authors.


1365313x, 0, Downloaded from https://onlinelibrary.wiley.com/doi/10.1111/tpj.16742 by Institution Nac De Investig Tec Agra, Wiley Online Library on [24/05/2024]. See the Terms and Conditions (https://onlinelibrary.wiley.com/terms-and-conditions) on Wiley Online Library for rules of use; OA articles are governed by the applicable Creative Commons License